U.S. DEPARTMENT OF ENERGY | Office of Science

DOE/SC-ARM-23-011

Cloud and Precipitation Experiment at Kennaook (Cape-K) Science Plan

G Mace
M Keywood
R Humphries
C McCluskey
Y Huang
P-L Ma
R Marchand
A Protat
S Fiddes
S Siems
P May

June 2023

ARM

DISCLAIMER

DOE/SC-ARM-23-011

Cloud and Precipitation Experiment at Kennaook (Cape-K) Science Plan

G Mace, University of Utah
R Marchand, University of Washington
Principal Investigators

M Keywood, Commonwealth Science and Industrial Research Organisation (CSIRO)
A Protat, Bureau of Meteorology
R Humphries, CSIRO
S Fiddes, Australian Antarctic Program Partnership, University of Tasmania
C McCluskey, National Center for Atmospheric Research
S Siems, Monash University (MU)
Y Huang, University of Melbourne
P May, MU
P-L Ma, Pacific Northwest National Laboratory
Co-Investigators

June 2023

How to cite this document:

Mace, J, R Marchand, M Keywood, A Protat, R Humphries, S Fiddes, C McCluskey, S Siems, Y Huang, P May, and P-L Ma. 2023. Cloud and Precipitation Experiment at Kennaook (Cape-K) Science Plan. U.S. Department of Energy, Atmospheric Radiation Measurement user facility, Richland, Washington. DOE/SC-ARM-23-011.

Work supported by the U.S. Department of Energy,
Office of Science, Office of Biological and Environmental Research

Executive Summary

The Cloud and Precipitation Experiment at Kennaook[1] (CAPE-K) will augment ongoing measurements at the Kennaook/Cape Grim Baseline Air Pollution Station (KCG) with components of the U.S. Department of Energy Atmospheric Radiation Measurement (ARM) user facility's second Mobile Facility (AMF2) in a deployment that is scheduled to extend from April 2024 through September 2025. Located at Kennaook/Cape Grim on the northwestern tip of Tasmania (40.68º S, 144.69º E), KCG has produced the longest and most consequential record of Southern Hemisphere aerosol and gas-phase chemistry; however, extensive cloud and precipitation measurements have not been collected at this site.

CAPE-K is motivated by the fact that model uncertainty in the surface radiation budget due to clouds and precipitation remain significant in this region, where strong latitudinal gradients in cloud feedbacks are found and there are strong and well-documented seasonal variations in marine aerosol properties. Satellite data suggest that cloud properties co-vary with the seasonal cycle in aerosol in the Southern Ocean (SO), yet detailed vertically resolved measurements of cloud and precipitation in the marine boundary layer are sparse. CAPE-K will provide the first such seasonal cycle of measurements in this important latitude band. CAPE-K will provide detailed cloud and precipitation observations over two winter seasons and align with complementary high-value-add activities planned by Australian colleagues, including a voyage of the Research Vessel *Investigator* (RVI) in May 2025 that will conduct measurements just offshore of KCG.

We identify three science objectives that the CAPE-K deployment will enable:

1. Document the seasonal cycle of SO low-cloud and precipitation properties and associated surface radiative fluxes, and examine how these properties co-vary with dynamical and thermodynamical factors, and aerosol (cloud condensation nuclei; CCN) concentrations and composition.
2. Compare and contrast these relationships with observations from other surface sites and campaigns including other ARM sites and research voyage data sets.
3. Study aerosol-cloud-precipitation interactions in pristine marine low clouds and explore how these interactions can best be represented in models at various scales.

Pursuit of these objectives will be enabled by deployment of a subset of AMF2 instruments to the KCG site that feature vertically pointing cloud remote-sensing instruments, as well as radiosonde, surface meteorological, and radiation instrumentation. We plan to conduct four intensive operational periods (IOPs) during the CAPE-K deployment. These IOPs will consist of one-month periods when high-time-resolution radiosondes will be deployed when the air mass trajectories are from the southwest.

[1] Kennaook/Cape Grim, Tasmania. 40.68° S, 144.69° E. (Note: Cape Grim has recently been renamed to recognize the traditional ownership of the land. A dual name, Kennaook/Cape Grim, has been adopted and its use in the both the scientific and general community is being actively encouraged.)

Acronyms and Abbreviations

ACCESS	Australian Community Climate and Earth System Simulator
AMF	ARM Mobile Facility
ANSTO	Australian Nuclear Science and Technology Organization
AOS	Aerosol Observing System
APS	aerodynamic particle sizer
ARM	Atmospheric Radiation Measurement
ASR	Atmospheric System Research
AWARE	ARM West Antarctic Radiation Experiment
BAMS	*Bulletin of the American Meteorological Society*
BOM	Bureau of Meteorology
CALIPSO	Cloud-Aerosol Lidar and Infrared Pathfinder Satellite Observations
CAM	site-monitoring camera
CAPE-K	Cloud and Precipitation Experiment at Kennaook
CAPRICORN	Clouds, Aerosols, Precipitation, Radiation, and Atmospheric Composition over the Southern Ocean
CCN	cloud condensation nuclei
CDC	cloud drop concentration
CEIL	ceilometer
CER	cloud effective radius
CESM	Community Earth System Model
CLUBB	Cloud Layers Unified By Binormals
CLWP	cloud liquid water path
CMIP5	Coupled Model Intercomparison Project phase 5
CMIP6	Coupled Model Intercomparison Project phase 6
CN	condensation nuclei
COMBLE	Cold-Air Outbreaks in the Marine Boundary Layer Experiment
CSIRO	Commonwealth Science and Industrial Research Organisation
CS-PHOT	Cimel sun photometer
CTT	cloud top temperature
DMS	dimethylsulfide
DQPR	Data Quality Problem Reporting
E3SM	Energy Exascale Earth System Model
ECMWF	European Centre for Medium-Range Weather Forecasts
ENA	Eastern North Atlantic
ERA5	fifth-generation ECMWF atmospheric reanalysis of the global climate

FT	free troposphere
GAW	Global Atmosphere Watch
GCM	global climate model
HTDMA	humidified tandem differential mobility analyzer
IFS	Integrated Forecast System
INP	ice-nucleating particle
IOP	intensive operational period
IR	infrared
IRT	infrared thermometer
ISCCP	International Satellite Cloud Climatology Project
KAZR	Ka-band ARM Zenith Radar
KCG	Kennaook/Cape Grim Baseline Air Pollution Station
LDIS	laser disdrometer
LES	large-eddy simulation
LWP	liquid water path
MAERI	marine atmospheric emitted radiation interferometer
MARCUS	Measurements of Aerosols, Radiation, and Clouds over the Southern Ocean
MBL	marine boundary layer
MFR	multifilter radiometer
MFRSR	multifilter rotating shadowband radiometer
MG3	third-generation Morrison-Gettelman microphysics scheme
MICRE	Macquarie Island Cloud and Radiation Experiment
MODIS	Moderate Resolution Imaging Spectroradiometer
MPL	micropulse lidar
MU	Monash University
MWACR	Marine W-band ARM Cloud Radar
MWR	microwave radiometer
MWR-2C	microwave radiometer, 2-channel
MWR-3C	microwave radiometer, 3-channel
NCAR	National Center for Atmospheric Research
NSA	North Slope of Alaska
OPC	optical particle counter
ORG	optical rain gauge
PDF	probability density function
PI	principal investigator
PICCAASO	Partnerships for Investigating Clouds and the bioChemistry of the Atmosphere in Antarctica and the Southern Ocean
POPS	persistent organic pollutants

PSAP	particle soot absorption photometer
PWD	present weather detector
PWV	precipitable water vapor
RRM	Regionally Refined Mesh
RVI	Research Vessel *Investigator*
RWP	radar wind profiler
SGP	Southern Great Plains
SH	Southern Hemisphere
SKYRAD	sky radiometer
SO	Southern Ocean
SOCEX	Southern Ocean Cloud Experiment
SOCRATES	Southern Ocean Clouds, Radiation, Aerosol Transport Experimental Study
SONDE	balloon-borne sounding system
SP2	single-particle soot photometer
SW	shortwave
TBERG	tipping bucket rain gauge
TSI	total sky imager
UHSAS	ultra-high-sensitivity aerosol spectrometer
UPS	uninterruptible power supply
UV	ultraviolet
VAP	value-added product
VDIS	video disdrometer
WMO	World Meteorological Organization

Contents

Figures

Tables

1.0 Background

Low-altitude clouds with layer-tops in or near the marine boundary layer (hereafter low clouds) are ubiquitous over the mid-latitude oceans (Woods 2012), impose a significant influence on the climate system (Tselioudis et al. 2021), and are difficult to accurately represent in climate models (Forbes and Ahlgrim 2014). The properties of these clouds are very sensitive to marine aerosol and the local dynamics and thermodynamics of the marine boundary layer (MBL). Marine aerosols are of global importance, impacting the Earth's radiative budget, biogeochemical cycling, ecosystems, and regional air quality (Carslaw et al. 2010). At present, uncertainties in our understanding of aerosols in the preindustrial environment limit our ability to quantify the radiative forcing due to anthropogenic aerosols since industrialization (Carslaw et al. 2014, Ghan et al. 2013). Over the SO, model studies suggest that anthropogenic aerosol forcing is small. The SO therefore has the potential to serve as a modern surrogate for aerosol-cloud interaction in the preindustrial era and offers a critical test case for climate model simulations of aerosols and aerosol-cloud interactions both for liquid and mixed-phase clouds, especially as regards the role of marine biogenic aerosols and their precursors (Korhonen et al. 2008, Kooperman et al. 2012).

Climate models participating in the most recent Coupled Model Intercomparison Project phase 6 (CMIP6) simulate strong latitudinal gradients in the response of low clouds to increases in greenhouse gases in the Southern Hemisphere high and mid-latitudes; see the top panel of Figure 1 (taken from Zenlinka et al. 2020).

In CMIP6, uncertainty in the low-cloud feedback remains the largest source of intermodel spread in warming (climate sensitivity) and is significantly more positive at the latitude of Kennaook/Cape Grim (40º S) than at any other latitude on Earth.

The strong gradients in shortwave low-cloud feedback components in the southern mid-latitudes are driven primarily by opposing changes in low-cloud amount and low-cloud optical depth (Zelinka et al. 2016, 2020, see lower two panels of Figure 1). Poleward of about 50º S, there is a relatively strong increase in the mean cloud optical depth with warming that causes an increase in solar radiation reflected to space (for a fixed cloud amount). This low-cloud optical depth response acts to reduce climate warming, constituting a negative feedback. The increase in cloud optical depth with warming is thought to be driven by an increase in cloud liquid water and cloud element longevity (that results from less rapid depletion of cloud water by precipitation processes due to a reduction in mixed-phase processes) (Ceppi et al. 2016, Terai et al. 2019).

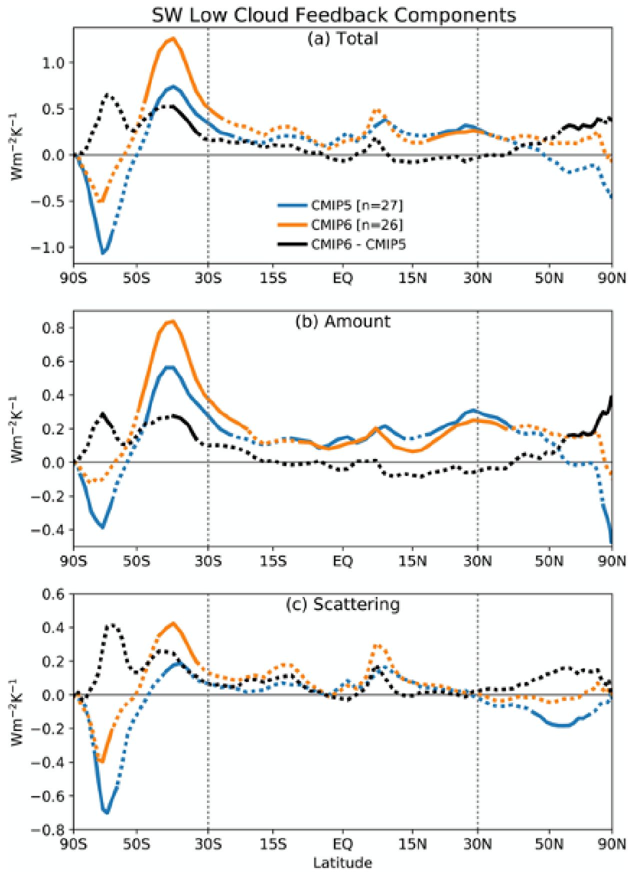

Figure 1. (a) Zonal mean SW low-cloud feedback and its breakdown into (b) amount and (c) scattering components for the (blue) CMIP5 and (orange) CMIP6 multimodel means. Latitudes where at least 80% of the models agree on the sign of the feedback are plotted with a solid line. Multimodel mean differences are shown in black lines, which are solid where differences are significant ($p < 0.05$). Results are plotted against the sine of latitude to display uniform area weighting. The red line highlights the latitude of KCG. Figure taken from Zenlinka et al. (2020).

Equatorward of about 50º S, there are larger reductions in low-cloud amount than poleward of 50º S. This reduces solar radiation reflected back to space and amplifies climate warming, thus constituting a positive feedback. We note that the total low-cloud shortwave (SW) feedback has more than doubled in the CMIP6 multi-model mean in the 50° S-30° S latitude domain, with most of this due to models having larger reductions in cloud amount with increasing temperature. KCG lies at the latitude where the SW cloud feedbacks reach their most positive point.

However, there is considerable uncertainty about the strength of these feedbacks and their overall balance (Wang et al. 2021). Mülmenstädt et al. (2021), for example, argue that the well-known bias in climate models for warm clouds to precipitate too readily causes an underestimate in cloud lifetime. This results in low-cloud feedbacks that are too positive in climate models for warm clouds, and this is especially pernicious in the Southern Hemisphere (SH) mid-latitudes because the error grows in importance with a reduction in mixed-phase clouds as the climate warms. More generally, uncertainties in the representation of aerosol-cloud-precipitation interactions remains high. For the SO, in particular, there are strong seasonal and latitudinal variations in cloud properties (McCoy et al. 2014) that correlate with seasonal and latitudinal variability in aerosols (Ayers and Gras 1991, Gras and Keywood 2017, Humphries et al. 2021) and which, in turn, depend on seasonality in biological activity (McCoy et al. 2015, Mace and Avey 2017, Twohy et al. 2021).

How various low-cloud feedbacks, both positive and negative, balance and compete in nature and are affected by seasonally varying aerosols over the SO is not well established, yet the result of these interactions is critical to our understanding of the Earth's climate sensitivity (Tan et al. 2016, Gettelman et al. 2020, Kay et al. 2016). CAPE-K will address these scientific issues by providing a multi-seasonal aerosol-cloud-precipitation data set that samples pristine Southern Ocean air masses.

2.0 Kennaook/Cape Grim Baseline Air Pollution Station (KCG)

The KCG Baseline Air Pollution Station (Figures 2, 3), is located in northwest Tasmania, Australia (latitude: 40° 41', 40.68° S; longitude: 144° 41', 144.69° E) on coastal bluffs overlooking the Southern Ocean. KCG was established in 1976 to monitor and study global atmospheric composition and has been in continuous operation for more than 45 years. The station is managed by the Bureau of Meteorology (BOM), with science leadership provided by the Commonwealth Science and Industrial Research Organisation (CSIRO), the University of Wollongong, and the Australian Nuclear Science and Technology Organization (ANSTO). KCG is one of three premier stations of the World Meteorological Organization (WMO) Global Atmosphere Watch (GAW) Program and is Australia's principal contribution to this international network that monitors changes in the earth's atmosphere.

Figure 2. Aerial view of the KCG looking towards the south. The station and tower can be seen in the bottom right of the image.

At KCG, long-term measurements are made of aerosol microphysical, optical, and chemical properties, reactive gases including tropospheric ozone, greenhouse gases, ozone depleting chemicals, radon (an indicator of recent terrestrial influences), solar radiation, rainfall chemical composition, mercury, persistent organic pollutants (POPS), and meteorological variables such as wind speed and direction, rainfall, temperature, humidity, air pressure, and boundary-layer height.

The observations made at KCG serve several purposes. They contribute objective evidence for policymakers who develop and monitor the effectiveness of international environmental agreements, which aim to achieve sustainable development. For example, KCG measurements of ozone-depleting chemicals have tracked the efficacy of the Montreal Protocol on Substances that Deplete the Ozone Layer (e.g., Montza et al. 2021), and they provide data and information that are used to elucidate, parameterize, and evaluate relevant processes in Earth system models such as aerosol and ozone formation, transformation, and removal in the remote marine boundary layer (e.g., Luhar et al. 2018).

Observations at KCG are particularly important as they provide a window to the SO, which is most likely the closest representation of natural atmosphere on the globe due to relatively minimal impact of anthropogenic sources. The occurrence of air masses passing over KCG from directions between 180° and 290° that have long trajectories over open water occur ~50% of the time. The occurrence of air masses with values of radon that would indicate little to no recent continental exposure (known as baseline conditions) occur ~30% of the time, with June and July having the most frequent baseline conditions.

The goal of aerosol observations at KCG has been to investigate the nature, sources, and processes of production and evolution of climatically important particles over the SO. This involves the characterization of SO marine boundary-layer aerosol and the processes that relate aerosol to climate change, investigating trends in long-term data sets (particles and gaseous elemental mercury), and collecting data that will lead to the improvement/assessment of aerosol and multiphase atmospheric chemistry schemes in models, including the role of aerosols in cloud formation and regulation.

Data sets from KCG show there is a strong seasonal cycle in aerosol properties, including cloud condensation nuclei (CCN; Ayers and Gras 1991) and cloud droplet number concentrations (Boers et al. 1998), with the lowest concentrations observed in the winter and highest in the summer. While the summer peak is likely due to marine biogenic sources, the process pathways remain uncertain (Quinn and Bates 2011) and climate models fail to simulate the mean annual and seasonal cycle of CCN and cloud droplet concentrations over the SO. Gras and Keywood (2017), using long-term condensation nuclei (CN) and aerosol composition data from KCG, suggest that dimethylsulfide (DMS) oxidation is only a significant source of CCN during the warm months.

Marine (SO) aerosol sources include primary sea-spray emissions composed of both sea salt and biogenic organic components (Quinn et al. 2014) and biogenic gas-phase aerosol precursors, including DMS and organic species. Korhonen et al. (2008) suggested through modeling that DMS oxidation products nucleate to form new particles in the free troposphere (FT) before being transported or subsiding back to the marine boundary layer (MBL) to act as CCN. Observations support the FT being an important aerosol pathway over the SO during the summer (Gras 2009, Kang et al. 2022).

A strong driver for aerosol and radiation observation programs at KCG is to contribute information that will lead to a reduction in the SO radiative bias present in our climate and weather models, which has been attributed to the incorrect simulation of cloud frequency and phase over the SO (Fiddes et al. 2022). However, the lack of co-located cloud and precipitation observations at KCG makes this objective difficult to address. The deployment of the ARM facility at KCG will provide invaluable data that can connect the decades of aerosol measurements with cloud properties and processes.

3.0 Science Objectives of CAPE-K

The scientific rational for CAPE-K is linked to measurements of pristine marine air masses that pass over the region following long trajectories over the SO. As described in Section 2, we refer to this as baseline air (Figure 3). Baseline air often arrives at the KCG site in the cold air advection behind mid-latitude cyclones and has specific boundary-layer structure that features marine inversions and varying levels of thermodynamic instability. Thus, our focus is on the interaction between open- and closed-cell stratocumulus clouds and the role of aerosol and precipitation in shaping the life cycles of these clouds. Our science objectives follow from this understanding.

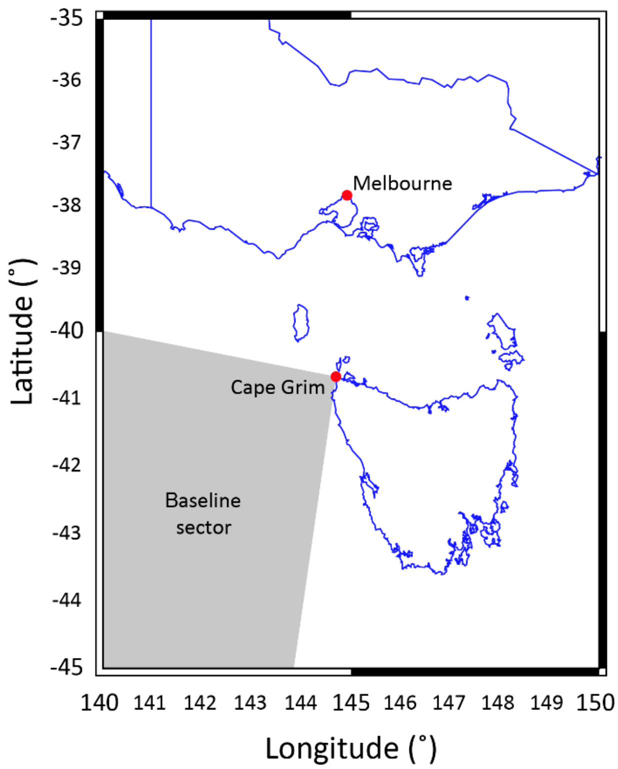

Figure 3. From Gras and Keywood (2017) showing the location of Kennaook/Cape Grim and the baseline sector from which pristine airmasses are observed.

Objective 1: Document the seasonal cycle of SO low-cloud and precipitation properties and associated surface radiative fluxes, and examine how these properties co-vary with dynamical and thermodynamical factors, and aerosol (CCN) concentrations and composition.

A key motivation for the proposed experiment is to quantify how cloud and precipitation properties vary seasonally within the context of seasonal oscillations in atmospheric state and ambient aerosol. Specific cloud and precipitation properties that will be examined include SO low-cloud and precipitation occurrence, phase, and microphysics parameters that define or constrain the particle size distribution (such as the number concentration, effective radius, water content, width/shape factor). These cloud and precipitation properties will be determined along with the associated surface radiative fluxes and, more generally, variables that characterize the local atmospheric state and boundary-layer mesoscale structure.

There is a strong seasonal cycle in CCN and aerosol composition that is well documented at KCG (Ayers and Gras 1991, Gras and Keywood 2017). Figure 4 from Gras and Keywood (2017) show the aerosol seasonal cycle where CCN vary from several hundred cm^{-3} in the summer to several dozen cm^{-3} in the winter. The effect of the strong seasonal cycle in aerosols on satellite retrievals of cloud properties (especially cloud droplet number concentrations) is well established over the SO (McCoy et al. 2014, 2015; Mace and Avey 2017, Mace et al. 2023) and, as will be shown below, there are larger cloud droplet number concentrations and smaller cloud effective radii during the SH summer at KCG. The effect on precipitation is not as clear and is a topic of scientific interest for CAPE-K, but drizzle is less frequent during the summer.

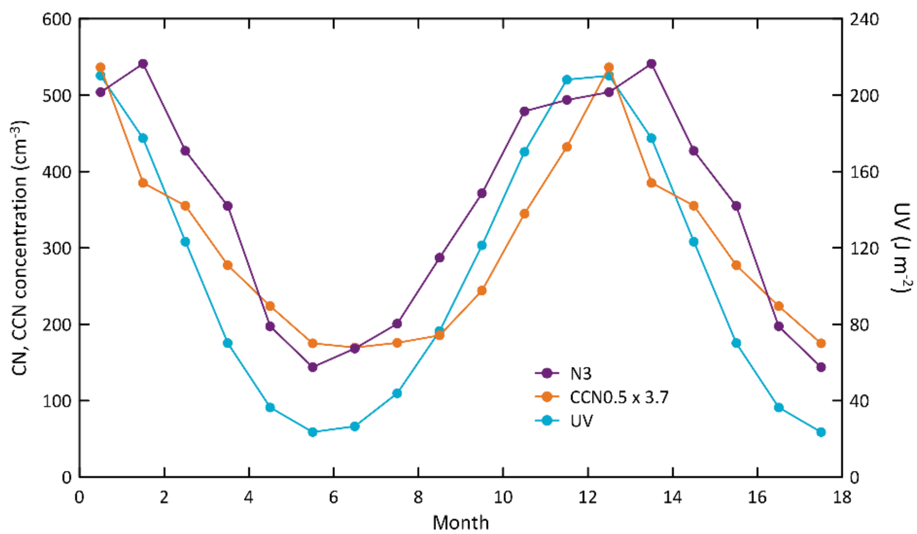

Figure 4. From Gras and Keywood (2017). Seasonal variation in N3 (aerosol concentration for particles larger than 3 nm), CCN at 0.5% supersaturation times 3.7 (during periods with low radon emissions indicative of airmasses having traveled over open ocean for an extended period), and UV radiation. N3 and UV data are from 1978-2005. CCN are monthly medians from 1981-2006. **Note:** CCN is multiplied by 3.7. Summer CCN peak is 135 cm^{-3} and winter minimum is ~55 cm^{-3}.

Given the strong seasonal cycle in aerosols, we expect that even basic observational statistics compiled from the measurements alone (radar contour frequency by altitude diagrams, for instance) will illustrate the extent of the coupling between aerosol and cloud properties over the seasonal cycle. As Boers et al. (1998) wrote in comparing aircraft data collected just upwind from the KCG during the Southern Ocean Cloud EXperiment (SOCEX) I and II (in 1993 and 1995, respectively), "The differences between summer and winter are so large that errors in sampling and measurement uncertainties hardly influence the results." We expect to find a similar contrast in the seasonal cycle of clouds at KCG while recognizing the challenge of isolating the cloud responses due to aerosols from those driven by temperature or other factors.

Many approaches can and have been taken by investigators to examine how aerosol, cloud, and precipitation co-vary. Given our focus on cloud feedbacks, we find the approach taken by Terai et al. (2019) to be particularly appealing. In their approach, Terai and co-authors examine the dependence of cloud properties on mean cloud temperature, defined as $d\ln(X)/dT$, where *ln* is the natural logarithm and X is a cloud property of interest (e.g., cloud optical depth τ, thickness h, effective radius Re, liquid water path LWP – all of which will be derived from ARM measurements), and T is the mean cloud temperature.

dln(X)/dT is obtained as the regression slope among hourly-mean samples between *ln(X)* and *T* in 15-K bins. Figure 5 shows an example of their results applied to optical depth at the ARM North Slope of Alaska (NSA), Southern Great Plains (SGP), and Eastern North Atlantic (ENA) sites using two retrievals for optical depth. The positive values of *dln(X)/dT* at temperatures less than about 0° C means there is an increase in optical depth (a negative cloud feedback) at these colder temperatures, while the negative values of *dln(X)/dT* at warmer temperatures means a decrease in optical depth (a positive feedback). The climate model results shown in the bottom panel of Figure 1 are conceptually consistent with Terai's results for the NSA, in the sense that they show an overall negative low-cloud optical depth feedback at cold temperatures (latitudes south of 50° S).

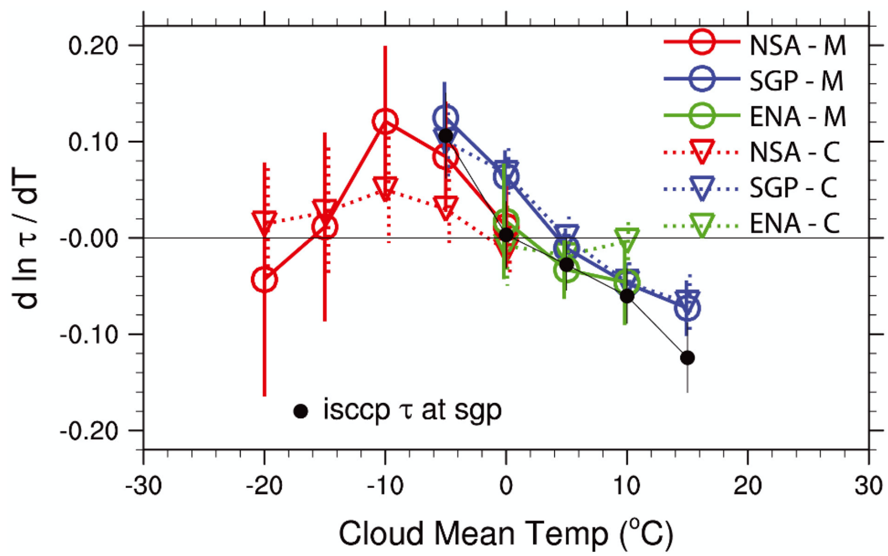

Figure 5. The sensitivity of cloud optical depth to cloud temperature, diagnosed as the derivative of the natural logarithm of low-cloud optical depth with respect to temperature as a function of temperature in 15-K cloud temperature bins. The cloud optical depth is from multifilter rotating shadowband radiometer (circles with solid lines) and micropulse lidar (upside-down triangles with dashed lines) retrievals at NSA (red), SGP (blue), and ENA (green) sites. Vertical lines accompanying each data point mark the 95% confidence interval for the regression slope *dln(τ)/dT*. Results from ISCCP satellite data at SGP are denoted by black solid dots. NSA = North Slope of Alaska; SGP = Southern Great Plains; ENA = Eastern North Atlantic; ISCCP = International Satellite Cloud Climatology Project. Figure taken from Terai et al. (2019).

The above approach can be applied to a variety of cloud and precipitation properties collected over the course of an annual cycle. Remaining cognizant of sample size, we envision this approach being applied at relatively high versus low aerosol concentrations (or indeed rotating the problem to examine aerosol and precipitation susceptibility, e.g., *dln(X)/d*(CCN), in different temperature ranges) and for some specific dynamical regimes (e.g., pristine airmass coming from deep SO latitudes based on back trajectories and/or radon levels). Other approaches to constraining aspects of the cloud-aerosol interactions can also be explored with the CAPE-K data set (e.g., Gryspeerdt et al. 2017, 2019).

To develop process-level understanding from observational statistics like those in Figure 5, it is necessary to account for covariances with other factors. Terai and co-authors, for example, perform a multilinear regression using the inversion strength, vertical humidity gradient, and degree of decoupling (again, all properties that we will measure as part of CAPE-K).

Investigators will be able to use the CAPE-K data sets to explore new approaches to study cloud feedbacks, aerosol-cloud interactions, and to quantify how cloud and precipitation properties co-vary with aerosol properties and environmental conditions. We mention the approaches of Terai et al. (2019) and Gryspeerdt et al. (2017, 2019) as illustrations of the type of analysis that CAPE-K will make possible.

Objective 2: Compare and contrast the cloud and precipitation properties (and relationships from Objective 1) with observations from other sites and campaigns.

A relatively simple but important way to gain insight into the processes that control low-cloud and precipitation properties, their feedbacks, and sensitivities to aerosols is through comparison of data from different locations. This is also important for the evaluation of climate models, which ultimately need to work well globally.

The analysis approach described in Objective 1 addresses this goal. We note, also, that the ARM SGP and ENA sites do not have much MBL clouds with mean temperatures below –5^{o} C, which are common at NSA and will be common at KCG during the winter season. In addition to the primary ARM sites, we also envision that **KCG will be compared with data from the DOE-sponsored Macquarie Island Cloud and Radiation Experiment (MICRE) and Measurements of Aerosols, Radiation, and Clouds over the Southern Ocean (MARCUS)** (and potentially other ARM/AMF sites/deployments, i.e., ARM West Antarctic Radiation Experiment [AWARE] and Cold-Air Outbreaks in the Marine Boundary Layer Experiment [COMBLE]) to obtain a more complete understanding of properties and processes over the SO.

Of particular interest is an increased understanding of the occurrence of mixed-phase processes and how this might differ at 40^{o} S relative to what has been observed further south in the SO, and how it might vary seasonally. As highlighted in recent papers by Mace and Protat (2018) and Mace et al. (2021b), the occurrence of mixed-phase processes in low clouds is higher than one would expect based on cloud-top phase retrievals from Cloud-Aerosol Lidar and Infrared Pathfinder Satellite Observations (CALIPSO; spaceborne lidar). The left panel in Figure 6 demonstrates that many low clouds that are identified as having supercooled liquid tops often have ice-phase precipitation falling from them. Over the SO, there appears to be a strong correspondence between the presence of ice and radar reflectivity factors more than –10 dBZe in cold-topped clouds.

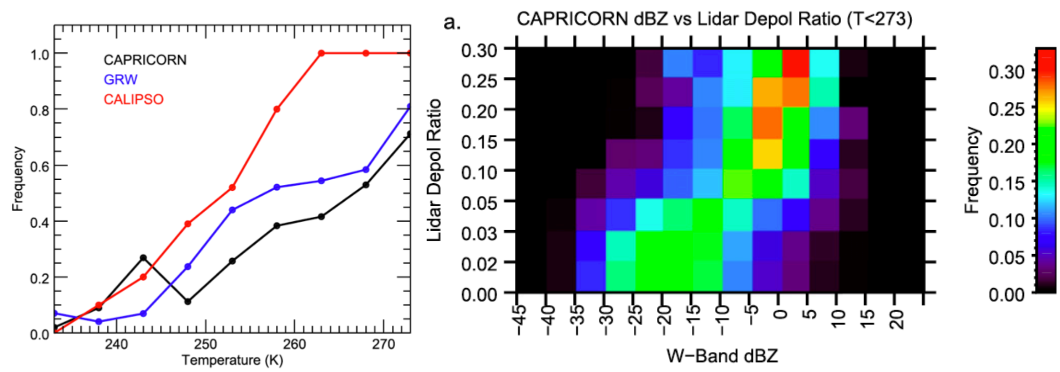

Figure 6. Left panel: Supercooled liquid fraction for Clouds, Aerosols, Precipitation, Radiation, and Atmospheric Composition over the Southern Ocean (CAPRICORN; black), Graciosa Island, Azores (GRW; blue), and(CALIPSO as reported by Hu et al. (2010) (red). CAPRICORN and GRW are fractions of data where ice is observed precipitating from the bottom of clouds (based on lidar depolarization), while CALIPSO is retrieved cloud-top phase. The lower values for CAPRICORN and GRW indicated that mixed-phase processes are active in clouds much more often than suggested by the CALIPSO phase retrieval. Right panel: Distributions of linear depolarization ratios for below-cloud precipitation in terms of W-band radar reflectivity. Depolarization ratios greater than 0.05 are indicative of ice precipitation. This panel show that reflectivity values larger than about –10 dBZ frequently have ice-phase precipitation. Normalization is performed across the rows of the histograms so that each row shows an independent frequency distribution. Panels from Mace and Protat (2018).

Objective 3: Study aerosol-cloud-precipitation interactions in low clouds and explore how these interactions can best be represented in models at various scales.

To obtain a better understanding of aerosol-cloud-precipitation interactions, and to test climate model parameterizations, investigators will be able to employ a variety of models from simple source-and-sink CCN budget models, to single-column models (SCMs) using parameterizations typical of climate models, to detailed large-eddy simulation (LES). Key to these activities is being able to prescribe the atmospheric state and forcing data for the model simulations. While reanalysis data can be used, such data products do not always capture the detailed thermodynamic structure of the boundary layer. Atlas et al. (2020), for example, found nudging to radiosonde data with their LES studies of SO clouds more closely matched observed cloud profiles than simulations nudged to fifth-generation European Centre for Medium-Range Weather Forecasts (ECMWF) atmospheric reanalysis of the global climate (ERA5) and focused on radiosonde-constrained simulations in their microphysical comparisons and sensitivity tests with stratiform clouds. In part to support case study modeling, we will conduct several intensive operational periods (IOPs), during which radiosondes will be launched every 3 to 6 hours. IOPs are discussed further in Section 4.6.

Studies using budget models, SCMs, and LES continue to be undertaken using MICRE, MARCUS, and Southern Ocean Clouds, Radiation, Aerosol Transport Experimental Study (SOCRATES) data sets, and a few examples are summarized below (Atlas et al. 2020, Zhou et al. 2021, Kang et al. 2022). In the longer term, we anticipate that simulations based on CAPE-K and these other experiments will be brought together into a larger framework for studying aerosol-cloud-precipitation interactions for the SO.

Atlas et al. (2020) examined several SOCRATES cases using a cloud-resolving LES and two coarse-resolution global atmospheric models. These authors found that the two-moment Morrison microphysics used in the LES simulated too few frozen particles in clouds occurring within the Hallett-Mossop temperature range. They obtained better simulation by tweaking the existing parameterization. While the nudged global climate models (GCMs) simulated reasonably well liquid-dominated mixed-phase clouds, in the stratiform cases they excessively glaciate cumulus clouds, and struggled to represent two-layer clouds (likely related to underpredicting stratiform cloud-driven turbulence).

Kang et al. (2022) applied the simple CCN budget model of Woods et al. (2012) to study coalescence scavenging in SO stratocumulus. These authors found coalescence scavenging is a dominant sink of CCN in both liquid- and mixed-phase precipitating stratocumulus and reduces the cloud droplet number concentration by as much as 90% depending on the precipitation rate. Gettelman and colleagues are comparing single-column-model simulations employing the third-generation Morrison-Gettelman (MG3) microphysics scheme and the Integrated Forecast System (IFS) microphysics scheme used operationally at ECMWF from June 2019 to June 2020 (manuscript in preparation). Overall, both schemes produce very low mean radiative biases but struggle to capture some individual low-cloud events correctly, and the overall low biases result from a cancellation of errors in different dynamical regimes.

4.0 CAPE-K Experimental Implementation

CAPE-K will augment ongoing measurements at KCG with components of the ARM AMF2 in a deployment that is scheduled to extend from April 2024 through September 2025. In this section we discuss operational aspects of CAPE-K including:

- ARM instruments and their prioritizations (Table 1, Sections 4.1, 4.1.1, 4.1.2)
- Instrument Calibration (Section 4.2)
- Instrument Operations (Section 4.3)
- Instrument Siting (Section 4.4)
- Daily Operations (Section 4.5)
- Intensive Operational Periods (Section 4.6)
- Retrievals and Value-Added-Products (Section 4.7)
- Guest Instruments and Collaborative Projects (Section 4.8)
- Data Management Plan (Section 4.9)

4.1 AMF2 Instrumentation

Meeting the science objectives will require continuous measurements of coincident aerosol, cloud, and precipitation micro- and macrophysical properties coupled with dynamical and thermodynamic information that characterizes the state of the boundary layer, with a primary focus on baseline conditions (when the atmospheric flow has long trajectories over the SO). Table 1 (below) summarizes the AMF instrumentation that will take part in CAPE-K.. Details follow in two subsections.

Table 1. AMF2 instrumentation for CAPE-K.

Instrument	Short name/system	Measurement	Priority
Ceilometer	CEIL	Cloud base height and attenuated backscatter	1-High
Doppler lidar	DL	Boundary-layer vertical motion	2-Moderate
Micropulse lidar	MPL/MPLPOLFS	Polarized attenuated backscatter profiles	1-High
Radiosonde	SONDE/BBSS	Thermodynamic and wind profiles	1-High
MAWS	MAWS	Meteorology station for MAWS	1-High
Surface meteorology	MET/MET	Surface temperature, relative humidity, surface pressure, wind direction and speed	1-High
Present weather detector	PWD/MET	Automated visibility, precipitation occurrence and type	1-High
Optical rain gauge	ORG/MET	Rain rate	1-High
Tipping bucket rain gauge	TBRG/MET	Rain rate	1-High
Laser disdrometer	LDIS(2)/LD	Precipitation type, rate, droplet properties	1-High
Tipping bucket rain gauge	WBPluvio/WB	Rain rate	2-Moderate
Ka-band zenith radar	KAZR/KAZR	Zenith Doppler spectra at Ka-band	1-High
W-band radar	MWACR/MWACR	Zenith Doppler spectra at W-band	1-High
Radar wind profiler	RWP/RWP	1290 GHz boundary-layer wind and radar reflectivity	2-Moderate
Marine atmospheric emitted radiation interferometer	MAERI/MAERI	Interferometric thermal infrared radiance	2-Moderate
CIMEL sun photometer	CSPHOT/CSPHOT	Shortwave narrowband radiances, aerosol optical depth, and Ångström exponent	3-Desired
Ground radiation	GNRAD/GNRAD	Upwelling shortwave and thermal infrared radiation	2-Moderate
Ground and sky infrared temperature	IRT-GND/IRT and IRT-SKY/IRT	Equivalent blackbody temperature from narrowband thermal IR	2-Moderate (sky) 3-Desired (gnd)
Multifilter radiometer	MFR/MFR	Narrowband hemispheric radiation at 415, 500, 615, 673, 870, and 940 nm	1-High
Multifilter rotating shadowband radiometer	MFRSR/MFRSR	Narrowband hemispheric and diffuse radiation at 415, 500, 615, 673, 870, and 940 nm	1-High
2-channel microwave radiometer	MWR-2C/MWR-2C	Liquid water path and precipitable vapor from 23.8 and 31 GHz zenith radiances	1-High

Instrument	Short name/system	Measurement	Priority
3-channel microwave radiometer	MWR-3C/MWR-3C	Liquid water path and precipitable vapor from 23.8, 30, and 89 GHz zenith radiance	1-High
Solar and infrared sky radiation	SKYRAD/SKYRAD	Downwelling solar and thermal IR hemispheric and direct normal radiances and irradiances	1-High
Total sky imager	TSI/TSI	Daytime hemispheric sky imagery and total cloud cover	1-High
Two-dimensional video disdrometer	VDIS/VDIS-(2DVD)	Drop sizes and fall velocity of precipitation	1-High
Cameras	CAM/CAM	Continuous imagery	1-High
Ice-nucleating particles	INP/INP	Ice-nucleating particle concentration from filter measurements	1-High
Aerodynamic particle sizer	APS/APS	Aerosol particle size spectrometer (0.3-20 microns)	1-High
Single particle soot photometer	SP@/SP2	Soot particle mass	2-Moderate
Ultra-high-sensitivity aerosol spectrometer	UHSAS/UHSAS	Aerosol size distribution 60 nm to 1 micron	1-High

4.1.1 Cloud and Precipitation Instrumentation

The deployment will include a suite of ARM remote and in situ sensors that will enable characterization of cloud and precipitation micro- and macrophysical properties. The instruments deemed critical for this category are the Ka-band ARM Zenith Radar (KAZR), the micropulse lidar (MPL), ceilometer (CEIL), microwave radiometer, 2-channel (MWR-2C), and balloon-borne sounding system (SONDE), as well as a variety of instruments that measure surface precipitation and (downwelling) radiation. The MWR-2C (and MWR-3C) will be used to constrain the integrated condensed liquid water and water vapor in the vertical column, while the MPL and CEIL provide critical information regarding cloud base height, phase, and other hydrometeor properties of the droplets and precipitation below and in the region just above cloud base. The MPL will also prove important to our understanding of the aerosol vertical structure in the boundary layer. The thermodynamic data provided by the SONDE are fundamental for many reasons, including providing critical thermodynamic information that will be needed to force models, characterize the boundary-layer vertical structure and inversion, and allow for the calculation (forward modeling) of gaseous absorption in MWR, radar, and other retrievals.

The surface meteorological measurements will also provide a record of variability in present weather conditions between sonde launches (as will the MWR for precipitable water), and surface precipitation (including measurements from the video disdrometer [VDIS], optical rain gauge [ORG], present weather detector [PWD], tipping bucket rain gauge [TBERG], and laser disdrometers [LDIS1 and LDIS2]) will be critical for understanding the vertical structure of precipitation. Other instruments in this category include those that provide data important for calibration of radar measurements and validation of retrievals. The situational awareness provided by the camera system (total sky imager [TSI] and site-monitoring camera

[CAM]) is always important as a visual record of the visible state of the sky and site during daylight hours. Radiation measurements (sky radiometer [SKYRAD], multifilter radiometer [MFR], multifilter rotating shadowband radiometer [MFRSR]) will provide radiative closure on the cloud property retrievals but also a record of how the clouds influence the downwelling radiative fluxes. Since ultimately understanding radiative forcing is at the center of our science objectives, it is necessary that the cloud properties retrieved from the combination of instruments be consistent with surface radiation.

The addition of the Marine W-band ARM Cloud Radar (MWACR), as a second independent radar frequency will significantly enhance the quality of precipitation property retrievals (because the reflectivity difference between the two radar bands provides information on the particles size for droplets larger than about ~300 microns). Other instruments listed as moderate priority in Table 1 will serve specific noncritical purposes (i.e., nice to have). For instance, the radar wind profiler (RWP) will allow for monitoring of boundary-layer winds and provide independent radar reflectivity at 1.3 GHz. The Cimel sun photometer (CS-PHOT) will provide aerosol optical depth information during periods when the solar disk is visible in addition to independent comparisons of precipitable water vapor (PWV). The marine atmospheric emitted radiation interferometer (MAERI) will provide constraints on the thermodynamic structure of the MBL and cloud-base characteristics, as can the up-looking infrared thermometer (IRT). Doppler lidar will provide important statistics on the three-dimensional boundary-layer winds. All of these will add to the value of the data set in various ways.

4.1.2 Aerosol Instrumentation

Since the KCG instrument suite provides comprehensive continuous measurements of aerosol properties, only a subset of the AMF2 Aerosol Observing System will be deployed for CAPE-K. These include the ultra-high-sensitivity aerosol spectrometer (UHSAS), APS, and single-particle soot photometer (SP2) instruments that complement or provide critical redundancy to the KCG measurements. In addition, ARM will deploy a guest instrument shelter with an aerosol inlet that will be sited near the KCG laboratory.

4.2 Instrumentation Calibration

Accurate calibration of the KAZR, MWACR, MPL, and MWR in particular and other instruments such as radiometers, disdrometers, etc. is critical to the inference of cloud and precipitation properties and the overall science goals of CAPE-K. Principal investigators (PIs) Mace and Marchand will work with the ARM infrastructure team and ARM instrument mentors to ensure that absolute calibration of the instruments will be conducted before and after CAPE-K, and to the degree possible, monitor the calibrations during the deployment as described below.

Regarding the radar calibration (at Ka- and W-bands), vicarious calibration based on periods with light rainfall (reflectivity <10 dBZe) and using disdrometer measurements combined with T-matrix calculation (Klepp et al. 2018) will be used to test the measured reflectivity, and as the opportunity presents, comparison with the EarthCARE spaceborne radar will also be conducted following Protat et al. (2022). The accuracy of radar Doppler velocities will be monitored vicariously through examination of velocity measurements at the tops of stratocumulus clouds (where the time-averaged Doppler velocities will be near zero).

The MPL and ceilometer calibration will be tested following the approach of O'Connor 2004, which examines the lidar ratios at the bases of optically thick clouds and adjusts calibration so that the mean lidar ratio is near 18.

Calibration of the MWR is also critical to the science objectives of CAPE-K. The calibration of the MWR is less of a concern given the long history of successful (and automated) use of tip curves in ARM. Nonetheless, the tip curve data will be monitored, and PI Marchand will pursue calibration using an external cold-target during IOPs.

Calibration of other instruments (e.g., broad band radiometers and sun photometers) will also follow standard ARM operating procedures to ensure the best possible data, with ARM radiative flux measurements also compared to satellite estimates, following Hinkelman and Marchand (2020).

4.3 Instrument Operations

CAPE-K science objectives focus on marine boundary clouds, aerosol-cloud interactions in low clouds, and precipitation; the modes of operation of some instruments will be targeted to optimally address the science objectives.

Radars: he millimeter radars (KAZR and MWACR) will focus their operational modes on the lower-tropospheric clouds (spending less time in modes designed to observe high-altitude clouds). In addition, the cycling of the radars through their modes needs to be coordinated to the extent possible so that data collection with the KAZR and MWACR is nearly simultaneous, with similar vertical range bins and similar dwell times. In addition, it will be critical to monitor the physical leveling of the radars so that the vertical beams are indeed vertical, and the measured Doppler vertical motion (and derived particle sedimentation velocities) are not contaminated by the typically strong horizontal winds.

MPL and MWR: We will explore the possibility of running the MWR and MPL in a high-temporal-resolution mode that will nominally be synchronous with the millimeter radar operations. The vertical structure of the MPL backscattering in the region just above cloud base has the potential to constrain cloud droplet number concentration when combined with the radars and the MWR. If possible, vertical resolutions of 1 to 5 meters would be optimal for the MPL for this microphysical retrieval purpose.

Radiosondes: Knowledge of the thermodynamic state of the MBL is critical information for the CAPE-K science objectives. During standard operational periods (non-IOP), two radiosondes will be launched per day by ARM personnel at the beginning and ending of the workday. Ideally, launches would occur every day. During periods of non-baseline conditions, this launch schedule could be relaxed. Radiosonde launches during IOP periods are addressed below.

INP filter samples: Ice-nucleating particle (INP) concentration at KCG will be determined from particles rinsed from filter samples. Such samples will be collected only during baseline conditions, and likely collected only during the day when ARM or KCG staff are present to determine if conditions warrant collection. Procedures for operation and swapping of filters will be develop over the coming year. Nonetheless, because INP concentrations over the SO are now known to be very low, it is possible and perhaps even likely that the KCG site will not be suitable for characterizing SO INP due to added contributions from the shore (or near-shore environment). Measurements collected from nearby ship (see section 4.8) will be critical to the evaluation of these INP data.

The operation of other instruments should be according standing operating procedures.

4.4 Instrument Siting

The AMF2 instrumentation will be deployed as depicted in Figure 7. The main set of sea containers will occupy a location approximately 200 m from the KCG facility along a local access road. Siting of radiometers will be nearby on a small hill to maximize the sky field of view. The AOS guest instrument shelter will be sited next to the KCG laboratory during the entire campaign.

Figure 7. Map of AMF2 instrument locations at KCG during CAPE-K. The drawn rectangles and red symbols indicate the locations of the sea containers and instruments.

4.5 Daily Operations

Nominally, all ARM instrumentation will be operating continuously once operations begin in April 2024. The PI team consisting of Mace, Marchand, and their students will begin monitoring datastreams and the local meteorology weekly. Of particular interest will be identification of baseline conditions. The PI team will keep an online public record of the meteorology at CAPE-K and quick-look data plots and preliminary cloud and precipitation property retrievals to ensure that the critical datastreams are of high quality. The PI team will also begin developing and keeping a record of observational and retrieval statistics so that errant or drifting datastreams can be identified quickly. The PI team will work closely with onsite ARM personnel and data quality personnel within ARM to ensure the highest-quality data set is produced from the CAPE-K deployment.

Radiosonde measurements will be critical for characterizing the state of the boundary layer. We plan to have two radiosonde launches per day with the idea that one sonde would be launched in the morning and one near the end of the workday. Two daily launches, 7 days per week, means that during non-IOP periods approximately 1,100 radiosondes will be launched during CAPE-K.

4.6 Intensive Operational Periods

IOPs will be held four times during CAPE-K. IOPs will be one-month periods with the main focus on baseline air conditions. The main feature of IOPs will be enhanced radiosonde launches (up to eight per day or three hourly) when in baseline conditions. We anticipate that, once scheduled, these IOPs would provide target periods for deployment of guest instrumentation to KCG and enhanced modeling activities. The scientific objective of an IOP would be to capture transitions in the mesoscale structure of low clouds during baseline conditions. Baseline conditions are typically associated with open-cellular cumulus (in unstable southwesterly flow) that often transition into closed-cell stratocumulus as the upstream surface ridge axis passes over KCG. Baseline conditions conclude when air mass trajectories shift to air sourced from continental Australia or Tasmania as the upstream warm frontal system approaches.

Climatologically, baseline conditions and the passage of synoptic-scale weather systems within which these cloud systems are embedded happen more frequently in winter than in summer, but are present in all seasons. Our goal is to capture at least two of these events in winter, summer, and spring. Spring is an interesting period because the CCN concentrations and composition are in the process of changing. Our nominal plan is to hold IOPs during June-July 2024, October-November 2024, January-February 2025, and May-June of 2025 (coinciding with the R/V *Investigator* voyage). Based on the climatology for the site, we expect 6 to 15 days in a month that might be suitable for intensive radiosonde launches. PIs Mace or Marchand and their students would be onsite during these periods to forecast and assist in launching radiosondes.

We expect that each of the cloud transitions will occupy several days to approximately one week. As our goal is to capture two such transitions in each IOP period, we would have 6-8 weeks of 3 hourly radiosonde launches during CAPE-K. With six additional radiosondes launched per day during this 6-8 week period, we anticipate using an additional 250-350 radiosondes for IOPs.

4.7 Retrievals and Value-Added Products

We are requesting that the following list of ARM value-added products (VAPs) be generated in support of the CAPE-K experiment. Here, the number in parenthesis indicates an attempt to prioritize the VAPS, but note that there is considerable flexibility in this regard, and we anticipate further planning and discussion with ARM translators as CAPE-K approaches.

Table 2. Requested ARM Cloud and Precipitation VAPs.

VAP acronym	VAP full name
KAZRARSCL (1)	Active Remote Sensing of CLouds (ARSCL) product for KAZR
MWACRARSCL (1)	W-band ARSCL
MICROARSCL (1)	Higher-order radar moments and features of Doppler spectra
MWRRET (1)	Improved MWR LWP/PWV Retrieval
AOD-MFRSR (2)	Aerosol Optical Depth (AOD) derived from MFRSR
MFRSRCLDOD (2)	Cloud Optical Properties from MFRSR Using Min Algorithm
MPLCOD (2)	Micropulse Lidar Cloud Optical Depth
INTERPSONDE (2)	Interpolated Sounding Data
RADFLUXANAL (2)	Radiative Flux Analysis
AERINF (2)	AERI Noise Filtered
AERIOE (2)	Thermodynamic Profile and Cloud Retrieval
DLPROF-WIND (3)	Doppler Lidar Horizontal Wind Profiles
LDQUANTS (3)	Laser Disdrometer Quantities
VDISQUANTS (3)	Video Disdrometer VAP

In addition to ARM VAPs, the PIs of CAPE-K (Mace and Marchand) will monitor data using a combination of routine measurement statistics and a few multi-instrument PI retrievals. We have found that such day-to-day monitoring by invested scientists and their students is critical to ensuring the highest-quality data sets are created from field programs like CAPE-K. While most of the instruments have a long tradition of use in ARM AMF deployments and the data quality monitoring by ARM has advanced greatly in recent years, problems that do not cause measured quantities to veer outside their normal ranges can be easily missed, especially if they involve subtle drifts.

Much of the PI monitoring will involve simple cross-instrument consistency checks, which ensure that measurements and retrievals are consistent with sky conditions. For example, is determination of cloud occurrence and cloud-base heights consistent between the MPL, ceilometer, and sky-imaging cameras? When the KZAR and MWACR data show non-precipitating liquid clouds are present, are the measured reflectivity factors the same (which should be true when particle sizes are small)? Is cloud thickness (based on radar and lidar), shortwave transmission, and MWR liquid water path consistent for low-level clouds, which are expected to be nearly adiabatic (see for example Kang et al. 2020)? When lightly precipitating warm cloud is present (that is, cloud whose cloud-top temperature is above 0^{o} C), are MPL depolarization ratios for the precipitation consistently near zero (which should be the case for spherical liquid particles)?

More complex checks will include the calibration test for the radar and lidar discussed in section 4.2, as well as the use of a few multi-instrument retrievals. Both the PIs have published algorithms that can be applied to the data. These algorithms have been developed mostly under ARM funding and applied to data collected in other SO campaigns. For instance, an algorithm that combines MWR, MPL, and W-Band radar to determine cloud droplet number concentration was published by Mace et al. (2021) and applied to data collected during MARCUS and CAPRICORN. This retrieval is sensitive to any inconstancy between the lidar backscattering and radar reflectivity. Likewise, Tansey et al. (2022)

examined the consistency of rain rate and particle size near the surface from radar reflectivity-velocity retrievals with surface disdrometer and tipping bucket measurements.

Combining datastreams in multi-instrument algorithms in near-real time will allow us to gain insight into data quality and will provide early indications of how the data are addressing the science objectives.

4.8 Guest Instruments and Collaborative Projects

The CAPE-K team welcomes collaborative projects that can add value to the CAPE-K data set from the international community.

In May of 2025, the Research Vessel *Investigator* (RVI) will conduct a voyage in support of KCG and CAPE-K (Co-Investigator Ruhi Humphries is lead investigator on that voyage). While the representativeness of the KCG to the wider SO atmospheric properties has been established to some degree by modeling and satellite studies, this voyage seeks to validate this finding using in situ aerosol and remote-sensing cloud observations. This voyage will be instrumented to make measurements similar to those at the station and will allow for comparison of the suite of observations of aerosol and cloud properties.

The RVI is Australia's flagship blue-water research vessel. The RVI hosts an extensive suite of instrumentation for the continuous observation of atmospheric chemistry, composition, and physics. This unique capability, modeled on the world-class capability at KCG, was recognized in 2018 as the world's first mobile platform in the WMO's GAW program. In addition to these permanent observations that comprise the vessel's GAW program, the RVI frequently hosts campaign-specific instrumentation, and to date, has undertaken more than 10 voyages with specific atmospherically focused research objectives. This has resulted in a rich marine atmospheric data set spanning a range of regions and seasons. See Mace and Protat (2018), Mace et al. (2021), and Humphries et al. (2021, 2023) for example studies conducted from data collected on the RVI.

A voyage has been scheduled in May 2025, coinciding with the proposed deployment period for the CAPE-K project. The RVI will station off KCG for ~one week so that direct comparisons can be conducted. Following this one-week period, the RVI will conduct an out-and-back transit along the mean flow to the SW to a minimum latitude of at least 52° S (Figure 8). Because the aerosol and cloud instrumentation on the RVI will broadly mimic the measurements at KCG, this voyage will provide significant value for CAPE-K. Not only will we be able to validate measurements through intercomparison, but the voyage data will allow us to test hypotheses regarding the representativeness of the CAPE-K measurements to the open ocean. We will also obtain correlative measurements in any cloud property gradients that may naturally exist in this region.

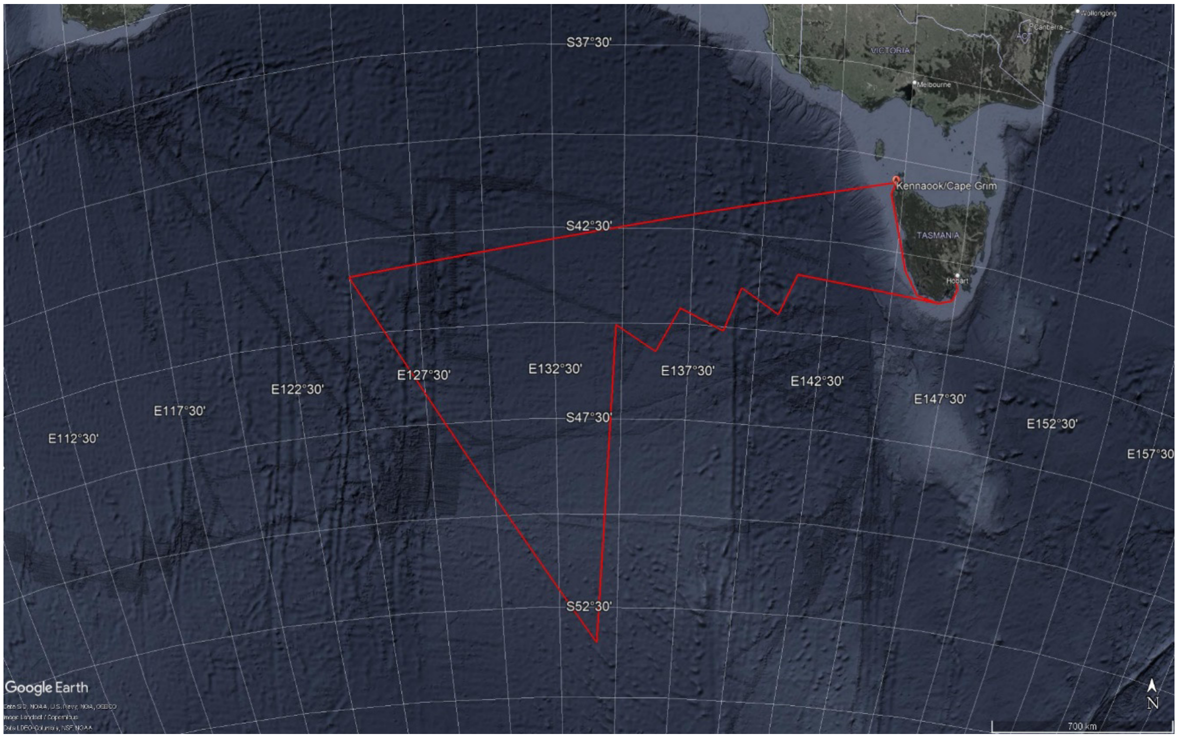

Figure 8. Proposed track of the Research Vessel *Investigator* during the July/August 2025 voyage to KCG. The transit to the southwest is to follow the mean streamline for baseline air. The track to the southeast is to sample into the winter Southern Ocean along southerly trajectories from KCG. The zig-zag pattern on return is to avoid ship exhaust contamination when traveling with the mean surface wind.

CI Protat plans to complement these aerosol observations with observations of clouds and precipitation measurements from a stabilized W-band cloud radar, cloud and aerosol backscatter lidar, micro rain radar, 2-channel microwave radiometer, and ODM470 disdrometer on RVI's mast to enable quantitative statistical comparisons between cloud and precipitation properties over the open ocean and at KCG. The RVI also operates a dual pol C-Band weather radar that will collect dual polarization precipitation measurements near and over KCG and all along the voyage track.

4.9 Data Management Plan

ARM data and VAPS, including those generated by the PIs, will follow ARM protocols that make all such data public shortly after collection via the ARM Data Center. The Australian community, including CSIRO and the BOM, which manage KCG and the data collected aboard the RVI, have their own data management policies that make all data public within a reasonable period of time following data collection (1 year) to ensure calibration and quality control.

PIs Mace and Marchand will communicate data quality problems to the ARM instrument mentors through the Data Quality Problem Reporting (DQPR) system, as they are identified, will review and report on data quality issues on a quarterly basis, and will produce a summary report for the entire experiment (to be posted on the ARM campaign web page associated with Cape-K), no later than three months after the conclusion of the experiment.

Following the experiment, an overview paper will be published in a widely read community journal, such as the *Bulletin of the American Meteorological Society* (BAMS). This paper will have public open access, in accordance with DOE requirements.

5.0 Management Plan

The roles and responsibilities of the Investigator Team are as follows:

PI Mace and Co-PI Marchand will work together to provide overall scientific leadership for CAPE-K and will liaise between ARM and the rest of the science team. Mace will have primary responsibility. Activities will include planning for CAPE-K, coordinating investigators, and monitoring ARM data to ensure that the datastreams being collected are of consistently high quality. PIs Mace and Marchand will also assist in the execution of IOPs and production of PI data products (Section 4.7). In addition, Drs. Mace and Marchand will provide outreach to the scientific community in order to socialize the CAPE-K data set. This will include an early experiment overview publication in a widely read community journal such as BAMS.

Co-I Keywood will lead the aerosol observations carried out at KCG during the ARM deployment and will contribute to the scientific analysis of the CAPE-K data set, with a focus on the aerosol microphysical, optical, and chemical properties. PI Keywood will also act as the scientific point of contact between the international project team and KCG.

Co-I Humphries will work with Co-I Keywood carrying out and undertaking the scientific analysis of the aerosol observations at KCG during the deployment. Co-I Humphries is also the Chief Scientist of the concurrent voyage aboard the RVI that will validate and expand the representativeness of the CAPE-K ARM deployment. In addition, his lead involvement with the Partnerships for Investigating Clouds and the bioChemistry of the Atmosphere in Antarctica and the Southern Ocean (PICCAASO) initiative will allow increased collaboration with relevant international scientists, and rapid uptake and reuse of data.

Co-I Protat will contribute to the data collection at KCG during IOPs, and will contribute to the scientific analysis of the CAPE-K data set, with a focus on the statistical properties of cloud and precipitation properties. He will contribute post-processed cloud radar, lidar, disdrometer, OceanPOL weather C-band dual-polarization Doppler radar, and micro rain radar measurements from the RVI. He will also provide access to post-processed data from the operational BOM West Takone C-band Doppler radar located about 90 km from KCG.

Co-I Dr. Christina McCluskey of the National Center for Atmospheric Research (NCAR) Climate and Global Dynamics Laboratory is working on improving the cloud parameterizations in the NCAR Community Earth System Model (CESM). She has participated in numerous investigations regarding SO cloud systems. In particular, she is very interested in the covariance among vertical motion and cloud properties that can be derived from Doppler spectra for the purpose of improving scale-aware parameterizations such as Cloud Layers Unified By Binormals (CLUBB).

Co-I Dr. Sonya Fiddes is working on improving the representation of clouds and aerosols in the Australian Community Climate and Earth System Simulator (ACCESS) model. She has worked closely with team members Protat and Humphries in using measurements to improve ACCESS. She will use the CAPE-K data to examine cloud and precipitation occurrence over the seasonal cycle in aerosol.

Co-I Dr. Yi Huang of the University of Melbourne is a widely published expert on cloud and precipitation over the SO using ground-based, aircraft, and satellite data. She will be an early user of the data for her research on SO clouds.

Co-I Dr. Steve Siems of Monash University will use the CAPE-K data set to examine how clouds and aerosols measured during CAPE-K will co-vary with the large-scale meteorology.

Co-I Dr. Peter May of Monash University is a widely published radar meteorology expert. He will assist the RVI team in interpreting the ARM radar measurements. In addition, he will seek support to deploy the Monash X-Band radar during the CAPE-K deployment.

Co-I Dr. Po-Lun Ma of the Pacific Northwest National Laboratory is working on improving the representation of aerosol and aerosol-cloud interactions for the next-generation Energy Exascale Earth System Model (E3SM). He has worked closely with Co-PI Marchand in using measurements to evaluate and improve E3SM using a kilometer-scale Regionally Refined Mesh (RRM) over the Southern Ocean. He will use the CAPE-K data to examine aerosol and aerosol-cloud-precipitation interactions.

6.0 Summary

There is considerable spread in current climate projections because of insufficient understanding of low-cloud feedbacks and aerosol-cloud-precipitation interactions over the SO. While much model radiative error in the previous generation of climate models (CMIP5) over the SO was due to errors associated with having too much cloud ice and not enough supercooled liquid water, and many climate models now produce more cloud composed of supercooled liquid water, the uncertainties remain consequential (Gettelman et al. 2019, Zelinka et al. 2020). As representative of this uncertainty, the magnitude of low-cloud feedback in the 40° S latitude range has nearly doubled between CMIP5 and CMIP6 (Figure 1). This change is due mostly to a greater reduction in cloud cover in CMIP6 in response to warming; while other recent studies suggest that the model's feedback is too positive in this latitude range as a result of producing too much precipitation in warm clouds (Mühlmenstädt et al. 2021). Such substantial disagreements in the modeling community suggest that climatologically meaningful observations are needed to better document the processes associated with cloud occurrence and precipitation in this latitude range.

Based on this science motivation, ARM is deploying components of the AMF2 to the KCG for a ~17-month period from May 2024 through September 2025 that we refer to as CAPE-K. The KCG observational facility has provided foundational aerosol measurements since the 1980s and provides access to cloud systems that exist in airmasses that have experience long trajectories over the pristine SO with minimal island influence. Large seasonal swings in CCN associated with the waxing and waning of biogenic precursor gases over the SO have been documented from KCG (~factor of 2.5 in monthly median CCN) in these pristine air masses. However, coincident cloud and precipitation measurements have not been made at KCG during this annual cycle in CCN, and the deployment of the ARM facility at KCG will provide invaluable data that can connect the decades of aerosol measurements with cloud properties and processes. Given this seasonal variability in natural marine aerosol, we contend that a collaborative data collection campaign that combines AMF components with the routine measurements at KCG has the potential to provide fundamentally new insights regarding aerosol-cloud-precipitation interaction over the Southern Hemisphere mid-latitudes in the precise latitude band where models are in most need of constraint. We note, in particular, that no detailed surface-based measurements of SO winter clouds have yet been collected at this latitude. CAPE-K will provide the first such measurements and will complement measurements collected further south in colder conditions during MICRE, MARCUS, and AWARE.

We have identified three science objectives that would be enabled by the CAPE-K deployment. These include comparing with other ARM datastreams collected in other locations and addressing modeling uncertainties. However, our primary objective is simply to document the seasonal cycle in cloud and precipitation occurrence, properties, and processes over this annual swing in marine aerosol. In the longer term, we expect the data will be at the core of process-level studies that enable a more detailed look at how clouds and precipitation co-vary in response to large changes in SO marine aerosol than is possible with the limited data that now exist.

Our project team consists of individuals with specific roles to play in the CAPE-K deployment, and we have identified several modeling and analysis experts in the U.S. and Australia who are very interested in early interaction with the CAPE-K data. This larger modeling and analysis team will be fully engaged in the planning and execution of CAPE-K, and we welcome participation by other members of the scientific community.

7.0 References

Ahn, E, Y Huang, ST Siems, and MJ Manton. 2018. "A comparison of cloud microphysical properties derived from MODIS and CALIPSO with in situ measurements over the wintertime Southern Ocean." *Journal of Geophysical Research − Atmospheres* 123(19): 11,120–11,140, https://doi.org/10.1029/2018JD028535

Andrews, E, PJ Sheridan, JA Ogren, D Hageman, A Jefferson, J Wendell, A Alastuey, L Alados-Arboledas, MH Bergin, M Ealo, AG Hallar, A Hoffer, I Kalapov, MD Keywood, J Kim, S-W Kim, F Kolonjari, C Labuschagne, N-H Lin, AM Macdonald, OL Mayol-Bracero, I McCubbin, M Pandolfi, F Reisen, S Sharma, JP Sherman, M Sorribas, and J Sun. 2019. "Overview of the NOAA/ESRL Federated Aerosol Network." *Bulletin of the American Meteorological Society* 100(1): 123−135, https://doi.org/10.1175/BAMS-D-17-0175.1

Atlas, RL, CS Bretherton, PN Blossey, A Gettelman, C Bardeen, P Lin, and Y Ming. 2020. "How well do large-eddy simulations and global climate models represent observed boundary layer structures and low clouds over the summertime Southern Ocean?" *Journal of Advances in Modeling Earth Systems* 12(11): e2020MS002205, https://doi.org/10.1029/2020ms002205

Ayers, GP, and JM Cainey. 2007. "The CLAW hypothesis: a review of the major developments." *Environmental Chemistry* 4(6): 366−374, https://doi.org/10.1071/EN07080

Ayers, GP, and JL Gras. 1991. "Seasonal Relationship between Cloud Condensation Nuclei and Aerosol Methanesulfonate in Marine Air." *Nature* 353(6347): 834−835, https://doi.org/10.1038/353834a0

Boers, R, JB Jensen, and PB Krummel. 1998. "Microphysical and short-wave radiative structure of stratocumulus clouds over the Southern Ocean: Summer results and seasonal differences." *Quarterly Journal of the Royal Meteorological Society* 124(545): 151−168, https://doi.org/10.1002/qj.49712454507

Carslaw KS, LA Lee, CL Reddington, KJ Pringle, A Rap, PM Forster, GW Mann, DV Spracklen, MT Woodhouse, LA Regayre, and JR Pierce. 2013. "Large contribution of natural aerosols to uncertainty in indirect forcing." *Nature* 503(7474): 67−71, https://doi.org/10.1038/nature12674. PMID: 24201280

Carslaw, KS, O Boucher, DV Spracklen, GW Mann, JGL Rae, S Woodward, and M Kulmala. 2010. "A review of natural aerosol interactions and feedbacks within the Earth system." *Atmospheric Chemistry and Physics* 10(4): 1701−1737, https://doi.org/10.5194/acp-10-1701-2010

Ceppi, P, DL Hartmann, and MJ Webb. 2016. "Mechanisms of the negative shortwave cloud feedback in high latitudes." *Journal of Climate* 29(1): 139–157, https://doi.org/10.1175/JCLI-D-15-0327.1

Chambers, SD, AG Williams, F Conen, AD Griffiths, S Reimann, M Steinbacher, PB Krummel, LP Steele, MV van der Schoot, IE Galbally, SB Molloy, and JE Barnes. 2016. "Towards a Universal "Baseline" Characterisation of Air Masses for High- and Low-Altitude Observing Stations Using Radon-222." *Aerosol and Air Quality Research* 16(3): 885–899, https://doi.org/10.4209/aaqr.2015.06.0391

Fiddes, SL, A Protat, MD Mallet, SP Alexander, and MT Woodhouse. 2022. "Southern Ocean cloud and shortwave radiation biases in a nudged climate model simulation: does the model ever get it right?" *Atmospheric Chemistry and Physics* 22: 14603–14630, https://doi.org/10.5194/acp-22-14603-2022

Forbes, RM, and M Ahlgrimm. 2014. "On the representation of high-latitude boundary layer mixed-phase cloud in the ECMWF global model." *Monthly Weather Review* 142(9): 3425–3445, https://doi.org/10.1175/MWR-D-13-00325.1

Galbally, IE, ST Bentley, and CPM Meyer. 2000. "Mid-latitude marine boundary-layer ozone destruction at visible sunrise observed at Cape Grim, Tasmania, 41°S." *Geophysical Research Letters* 27(23): 3841–3844, https://doi.org/10.1029/1999GL010943

Galbally, IE, AJ Miller, RD Hoy, S Ahmet, RC Joynt, and D Attwood. 1986. "Surface ozone at rural sites in the Latrobe Valley and Cape Grim, Australia." *Atmospheric Environment (1967)* 20(12): 2403–2422, https://doi.org/10.1016/0004-6981(86)90071-5

Gettelman, A, CG Bardeen, CS McCluskey, E Järvinen, J Stith, C Bretherton, G McFarquhar, C Twohy, J D'Alessandro, and W Wu. 2020. "Simulating observations of Southern Ocean clouds and implications for climate." *Journal of Geographical Research − Atmospheres* 125(21): e2020JD032619, https://doi.org/10.1029/2020JD032619

Ghan, SJ, SJ Smith, M Wang, K Zhang, KJ Pringle, KS Carslaw, J Pierce, S Bauer, and P Adams. 2013. "A simple model of global aerosol indirect effects." *Journal of Geophysical Research − Atmospheres* 118(12): 6688−6707, https://doi.org/10.1002/jgrd.50567

Gras, JL. 2009. "Postfrontal nanoparticles at Cape Grim: impact on cloud nuclei concentrations." *Environmental Chemistry* 6(6): 515−523, https://doi.org/10.1071/EN09076

Gras, JL, and S Whittlestone. 1992. "Radon and CN: Complementary tracers of polluted air masses at coastal and island sites." *Journal of Radioanalytical and Nuclear Chemistry Articles* 161(1): 293–306, https://doi.org/10.1007/BF02034903

Gras, JL, and M Keywood. 2017. "Cloud condensation nuclei over the Southern Ocean: wind dependence and seasonal cycles." *Atmospheric Chemistry and Physics* 17(7): 4419–4432, https://doi.org/10.5194/acp-17-4419-2017

Gryspeerdt E, T Goren, O Sourdeval, J Quaas, J Mülmenstädt, S Dipu, C Unglaub, A Gettelman, and M Christensen. 2019. "Constraining the aerosol influence on cloud liquid water path." *Atmospheric Chemistry and Physics* 19(8): 5331−5347, https://doi.org/10.5194/acp-19-5331-2019

Gryspeerdt, E, J Quaas, S Ferrachat, A Gettelman, S Ghan, U Lohmann, H Morrison, D Neubauer, DG Partridge, P Stier, T Takemura, H Wang, M Wang, and K Zhang. 2017. "Constraining the instantaneous aerosol influence on cloud albedo." *Proceedings of the National Academy of Sciences of the United States of America* 114(19): 4899−4904, https://doi.org/10.1073/pnas.1617765114

Hinkelman, LM, and R Marchand. 2020. "Evaluation of CERES and CloudSat surface radiative fluxes over Macquarie Island, the Southern Ocean." *Earth and Space Science* 7(9): e2020EA001224, https://doi.org/ 10.1029/2020EA001224

Humphries, RS, MD Keywood, S Gribben, IM McRobert, JP Ward, P Selleck, S Taylor, J Harnwell, C Flynn, GR Kulkarni, GG Mace, A Protat, SP Alexander, and G McFarquhar. 2021. "Southern Ocean latitudinal gradients of cloud condensation nuclei." *Atmospheric Chemistry and Physics* 21(16): 12757–12782, https://doi.org/10.5194/acp-21-12757-2021

Intergovernmental Panel on Climate Change. 2021. "Summary for Policymakers." In: *Climate Change 2021: The Physical Science Basis. Contribution of Working Group I to the Sixth Assessment Report of the Intergovernmental Panel on Climate Change*. Masson-Delmotte, V, P Zhai, A Pirani, SL Connors, C Péan, S Berger, N Caud, Y Chen, L Goldfarb, MI Gomis, M Huang, K Leitzell, E Lonnoy, JBR Matthews, TK Maycock, T Waterfield, O Yelekçi, R Yu, and B Zhou (eds.). Cambridge University Press, Cambridge, United Kingdom and New York, New York, pp. 3−32, https://doi.org/10.1017/9781009157896.001

Kang, L, RT Marchand, and WL Smith. 2021. "Evaluation of MODIS and Himawari-8 low clouds retrievals over the Southern Ocean with in situ measurements from the SOCRATES campaign." *Earth and Space Science* 8(3): e2020EA001397, https://doi.org/10.1029/2020EA001397

Kang, L, RT Marchand, R Wood, and IL McCoy. 2022. "Coalescence scavenging drives droplet number concentration in Southern Ocean low clouds." *Geophysical Research Letters* 49(7): e2022GL097819, https://doi.org/10.1029/2022GL097819

Kay, JE, C Wall, V Yettella, B Medeiros, C Hannay, P. Caldwell, and C Bitz. 2016. "Global climate impacts of fixing the Southern Ocean shortwave radiation bias in the Community Earth System Model (CESM)." *Journal of Climate* 29(12): 4617−4636, https://doi.org/10.1175/JCLI-D-15-0358.1

Keywood, MD. 2007. "Aerosol composition at Cape Grim: an evaluation of the PM10 sampling program and baseline event switches." In Cainey, JM, N Derek, and PB Krummel (Eds.). *Baseline Atmospheric Program Australia 2005-2006* (pp. 31–35). Melbourne: Australian Bureau of Meteorology and CSIRO Marine and Atmospheric Research.

Klepp, C, S Michel, A Protat, J Burdanowitz, N Albern, M Kähnert, A Dahl, V Louf, S Bakan, and SA Buehler. 2018. "OceanRAIN, a new in-situ shipboard global ocean surface-reference dataset of all water cycle components." *Scientific Data* 5(1): 180122, https://doi.org/10.1038/sdata.2018.122

Kooperman, GJ, MS Pritchard, SJ Ghan, M Wang, RCJ Somerville, and LM Russell. 2012. "Constraining the influence of natural variability to improve estimates of global aerosol indirect effects in a nudged version of the Community Atmosphere Model 5." *Journal of Geophysical Research − Atmospheres*, 117(D23): D23204, https://doi.org/10.1029/2012JD018588

Korhonen, H, KS Carslaw, DV Spracklen, GW Mann, and MT Woodhouse. 2008. "Influence of oceanic dimethyl sulfide emissions on cloud condensation nuclei concentrations and seasonality over the remote Southern Hemisphere oceans: A global model study." *Journal of Geophysical Research – Atmospheres* 113(D15): D15204, https://doi.org/10.1029/2007JD009718

Luhar, AK, MT Woodhouse, and IE Galbally. 2018. "A revised global ozone dry deposition estimate based on a new two-layer parameterisation for air-sea exchange and the multi-year MACC composition reanalysis." *Atmospheric Chemistry and Physics* 18(6): 4329−4348, https://doi.org/10.5194/acp-18-4329-2018

Mace, GG, S Benson, R Humphries, PM Gombert, and E Sterner. 2023. "Natural marine cloud brightening in the Southern Ocean." *Atmospheric Chemistry and Physics* 23(2): 1677–1685, https://doi.org/10.5194/acp-=23-1677-2023

Mace, GG, and A Protat. 2018. "Clouds over the Southern Ocean from the RV Investigator during CAPRICORN. Part 1: Cloud occurrence and phase partitioning." *Journal of Applied Meteorology and Climatology* 57(8): 1783−1803, https://doi.org/10.1175/JAMC-D-17-0194.1

Mace GG, and S Avey. 2017. "Seasonal variability of boundary layer cloud and precipitation properties in the Southern Oceans as diagnosed from A-Train Data." *Journal of Geophysical Research − Atmospheres* 122(2): 1015−1032, https://doi.org/10.1002/2016JD025348

Mace, GG, A Protat, RS Humphries, SP Alexander, IM McRobert, J Ward, P Selleck, M Keywood, and GM McFarquhar. (2021a). "Southern Ocean cloud properties derived from Capricorn and Marcus data." *Journal of Geophysical Research − Atmospheres* 126(4): e2020JD033368, https://doi.org/10.1029/2020jd033368

Mace, GG, A Protat, and S Benson. 2021b. "Mixed-phase clouds over the Southern Ocean as observed from satellite and surface-based lidar and radar." *Journal of Geophysical Research − Atmospheres* 126(16): e2021JD034569, https://doi.org/10.1029/2021JD034569

Marchand, R, and T Ackerman. 2010. "An analysis of cloud cover in multiscale modeling framework global climate model simulations using 4 and 1 km horizontal grids." *Journal of Geophysical Research – Atmospheres* 115(D16): D16207, https://doi.org/10.1029/2009JD013423

McCoy, DT, DL Hartmann, and DP Grosvenor. 2014. "Observed Southern Ocean cloud properties and shortwave reflection. Part I: Calculation of SW flux from observed cloud properties." *Journal of Climate* 27(23): 8836–8857, https://doi.org/10.1175/JCLI-D-14-00287.1

McCoy, DT, SM Burrows, R Wood, D-P Grosvenor, SM Elliott, P-L Ma, PJ Rasch, and DL Hartmann. 2015. "Natural aerosols explain seasonal and spatial patterns of Southern Ocean cloud albedo." *Science Advances* 1(6): e1500157–e1500157, https://doi.org/10.1126/sciadv.1500157

Molloy, SB, and IE Galbally. 2014. "Analysis and identification of a suitable baseline definition for tropospheric ozone at Cape Grim, Tasmania." In Derek, N, PB Krummel, and SJ Cleland (Eds.), *Baseline Atmospheric Program Australia 2009-2010* (pp. 7–16). Melbourne: Australian Bureau of Meteorology and CSIRO Marine and Atmospheric Research.

Montzka, SA, GS Dutton, RW Portmann, MP Chipperfield, S Davis, W Feng, AJ Manning, E Ray, M Rigby, BD Hall, C Siso, JD Nance, PB Krummel, J Mühle, D Young, S O'Doherty, P Salameh, C Harth, RG Prinn, RF Weiss, JW Elkins, H Walter-Terrinoni and C Theodoridi. 2021. "A decline in global CFC-11 emissions during 2018-2019." *Nature* 590: 428−432, https://doi.org/10.1038/s41586-021-03260-5

Mülmenstädt, J, M Salzmann, JE Kay, MD Zelinka, P-L Ma, C Nam, J Kretzschmar, S Hörnig, and J Quaas. 2021. "An underestimated negative cloud feedback from cloud lifetime changes." *Nature Climate Change* 11: 508–513, https://doi.org/10.1038/s41558-021-01038-1

Protat, A, V Louf, J Soderholm, J Brook, and W Ponsonby. 2022. "Three-way calibration checks using ground-based, ship-based, and spaceborne radars." *Atmospheric Measurement Techniques* 15(4): 915–926, https://doi.org/10.5194/amt-15-915-2022

Quinn, PK, and TS Bates. 2011. "The case against climate regulation via oceanic phytoplankton sulphur emissions." *Nature* 480(7375): 51−56, https://doi.org/10.1038/nature10580

Quinn, PK, DJ Coffman, JE Johnson, LM Upchurch, and TS Bates. 2017. "Small fraction of marine cloud condensation nuclei made up of sea spray aerosol." *Nature Geoscience* 10: 674–679, https://doi.org/10.1038/ ngeo3003

Scott, RC, TA Myers, JR Norris, MD Zelinka, SA Klein, M Sun, and DR Doelling. 2020. "Observed Sensitivity of Low-Cloud Radiative Effects to Meteorological Perturbations over the Global Oceans." *Journal of Climate* 33(18): 7717−7734, https://doi.org/10.1175/JCLI-D-19-1028.1

Tan, I, T Storelvmo, and MD Zelinka. 2016. "Observational constraints on mixed phase clouds imply higher climate sensitivity." *Science* 352(6282): 224−228, https://doi.org/10.1126/science.aad5300

Tansey, E, R Marchand, A Protat, SP Alexander, and S Ding. 2022. "Southern Ocean precipitation characteristics observed from CloudSat and ground instrumentation during the Macquarie Island Cloud and Radiation Experiment (MICRE): April 2016 to March 2017." *Journal of Geophysical Research − Atmospheres* 127(5): e2021JD035370, https://doi.org/10.102/2021JD035370

Terai, CR, Y Zhang, SA Klein, MD Zelinka, JC Chiu, and Q Min. 2019. "Mechanisms behind the extratropical stratiform low-cloud optical depth response to temperature in ARM site observations." *Journal of Geophysical Research − Atmospheres* 124(4): 2127–2147, https://doi.org/10.1029/2018JD029359

Tselioudis, G, WB Rossow, C Jakob, J Remillard, D Tropf, and Y Zhang. 2021. "Evaluation of clouds, radiation, and precipitation in CMIP6 models using global weather states derived from ISCCP-H cloud property data." *Journal of Climate* 34(17): 7311–7324, https://doi.org/10.1175/JCLI-D-21-0076.1

Twohy, CH, PJ DeMott, LM Russell, DW Toohey, B Rainwater, R Geiss, KJ Sanchez, S Lewis, GC Roberts, RS Humphries, CS McCluskey, KA Moore, PW Selleck, MD Keywood, JP Ward, and IM McRobert. 2021. "Cloud-nucleating particles over the Southern Ocean in a changing climate." *Earth's Future* 9(3): e2020EF001673, https://doi.org/10.1029/2020EF001673

Wang, C, BJ Soden, W Yang, and GA Vecchi. 2021. "Compensation between cloud feedback and aerosol-cloud interaction in CMIP6 models." *Geophysical Research Letters* 48(4): e2020GL091024, https://doi.org/10.1029/2020GL091024

Wood, R. 2012. "Stratocumulus Clouds." *Monthly Weather Review* 140(8): 2373–2423, https://doi.org/10.1175/MWR-D-11-00121.1

Zahorowski, W, IE Galbally, S Whittlestone, and CP Meyer. 1996. "Ozone and radon at Cape Grim: A study of their interdependence." In Francey, RJ, AL Dick, and N Derek (Eds.). *Baseline Atmospheric Program Australia 1993* (pp. 30–37). Melbourne: Department of the Environment, Sport and Territories, Bureau of Meteorology in cooperation with CSIRO Division of Atmospheric Research, Melbourne, Australia.

Zelinka,MD, C Zhou, and SA Klein. 2016. "Insights from a refined decomposition of cloud feedbacks." *Geophysical Research Letters* 43(17): 9259–9269, https://doi.org/10.1002/2016GL069917

Zelinka, MD, TA Myers, DT McCoy, S Po-Chedley, PM Caldwell, P Ceppi, SA Klein, and KE Taylor. 2020. "Causes of higher climate sensitivity in CMIP6 models." *Geophysical Research Letters* 47(1): e2019GL085782, https://doi.org/10.1029/2019GL085782

Zhou, X, R Atlas, IL McCoy, CS Bretherton, C Bardeen, A Gettelman, P Lin, and Y Ming. 2021. "Evaluation of cloud and precipitation simulations in CAM6 and AM4 using observations over the Southern Ocean." *Earth and Space Science* 8(2): e2020EA001241, https://doi.org/10.1029/2020EA001241

Appendix A

Representativeness of Kennaook/Cape Grim to the Open Ocean

A major assumption underpinning CAPE-K is that the cloud and precipitation properties that will be observed at KCG are consistent with those over the adjacent SO. Analysis of measurements of the atmospheric gas and aerosol composition at the site indicates that baseline air is sampled roughly half of the time in all months of the year (being somewhat more common in winter). This is important to CAPE-K as we are primarily interested in cloud and precipitation properties associated with pristine SO airmasses. Nonetheless, having airmasses with the same gas and aerosol composition as the pristine SO does not guarantee that the cloud and precipitation observed at the site will be uninfluenced by the island. The station sits on a bluff at the northwestern tip of Tasmania, and while the topography is lower in the northwest of the island as compared to that further south, we investigate if the island influences the properties of clouds and precipitation at the KCG location.

To assess the potential for differences in cloud and precipitation properties between the site and the adjacent ocean, we examine 20-year composites of Moderate Resolution Imaging Spectroradiometer (MODIS; satellite) cloud properties and three-year composites of C-band Doppler radar precipitation properties (collected from the weather radar located at West Takone, Tasmania). Our objective in this analysis is to determine if there are spatial gradients in cloud and precipitation properties that appear to be due to the island of Tasmania.

Figure 9 shows 20-year composite means for a variety of MODIS cloud retrievals restricted to periods when (50 m) winds at the station are coming from the west or south-west (between 190º and 280º clockwise from true N, see also Figure 3). The panels in the left column are for July (SH winter) and in right column for January (SH summer). These wind directions are typical of baseline conditions, but we note the data shown here have not been screened by aerosol properties or gas composition. The red square denotes the position of the station, and the panels in the top row show the total cloud fraction. Cloud occurrence is higher in winter (left panel) than summer (right panel). In both seasons, but more obvious in the winter, there is a reduction in cloud occurrence at the station as compared with the open ocean (~100 km further west) and notably lower cloud amounts to the east of the site in the lee of the island and along the northern coast. Toward the interior of the island, 50 to 100 km to the south and east, there is an increase in cloud occurrence associated with the higher topography.

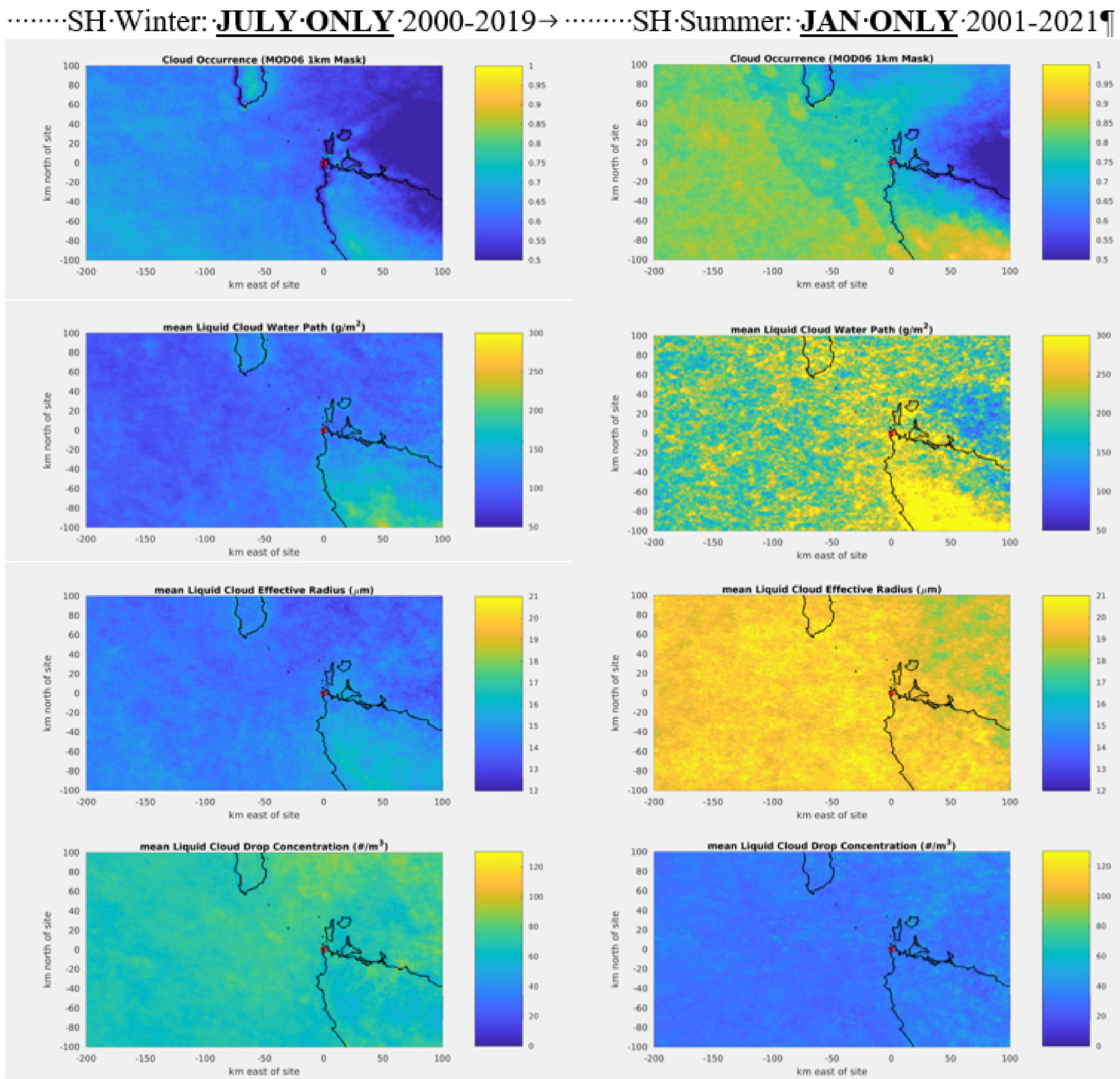

Figure 9. MODIS 20-year composite/mean cloud fields (50-m winds coming from 190° and 280°).

Likewise, there is a strong seasonal cycle in cloud top temperature (CTT; second row of panels), cloud liquid water path (CLWP; third row), liquid cloud effective radius (CER; fourth row), and liquid cloud drop concentration (CDC; bottom row). In both July and January, there are somewhat lower CTTs to the south and east of the site, and it may be that mean CTT at the site is very slightly cooler than over the adjacent ocean. The CLWP is significantly larger over the topography to the south and lower in the lee of the island (at least in July). In July (winter) the CLWP is significantly more variable than January (summer), which appears to be a result of the more frequent occurrence of open cellular mesoscale structures in winter (though we stress both open and closed [or overcast] structures are observed in both seasons). Overall, the data suggest there may also be a small increase in CLWP (when clouds are present) at the site and near the coast (within about 50 km of the coastline), at least in July. Spatial gradients in cloud effective radius and number concentration (bottom two rows), on the other hand, are even more subdued, and in all variables the spatial variations in the mean fields are much smaller than the seasonal differences.

Precipitation at KCG is observed by the BOM operational West Takone C-band Doppler radar. We have produced a spatial map of the rainfall frequency of occurrence using three winter seasons (2019-2021) of the operational rainfall product from the BOM (Rainfields3, Figure 10). Consistent with the cloud occurrence and CLWP, we find precipitation is more frequent over the Western Coast Range south of KCG and less frequent to the north of Tasmania. The rainfall occurrence at KCG appears to be like just off the coast, denoted by the boxes in the left panel of Figure 10. A comparison of rainfall rates (right panel of Figure 10) suggests that the distribution of precipitation rates is also similar, especially for the low rates typical of the shallow-cloud systems that are the focus of this proposal.

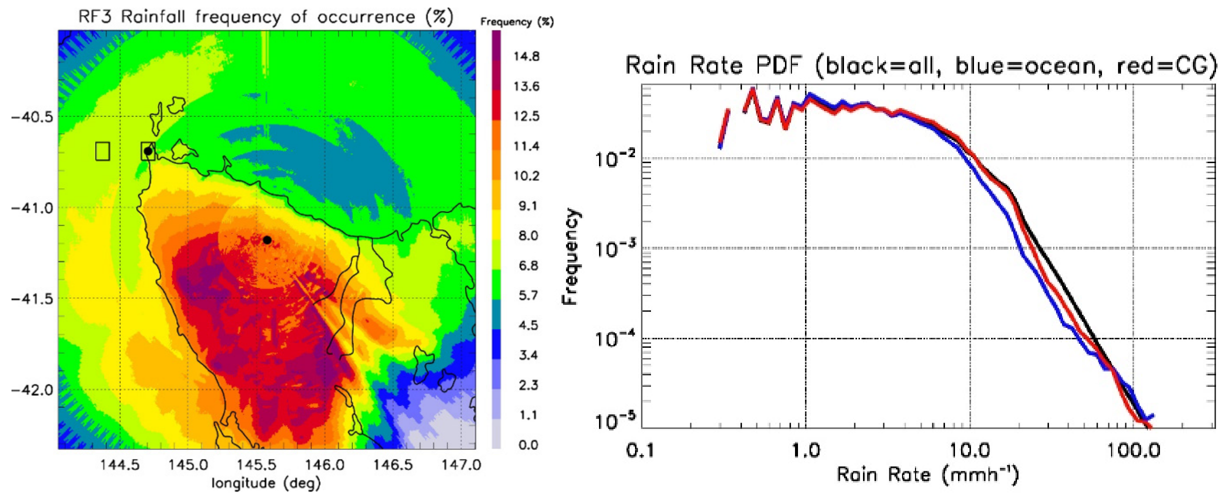

Figure 10. (left) Rainfall frequency of occurrence derived from three winters (JJA) of West Takone radar observations. Some artifacts (lines, circular rings) are observed, due to inaccurate vertical profile of reflectivity corrections near the radar (<30 km) and beam blocking in the southeastern part of the domain. These artifacts do not affect rainfall frequency in the vicinity of Cape Grim. The two boxes are those used to compare open ocean and Cape Grim rainfall PDFs in the right panel. (right) Rainfall rate probability density function (PDF) derived from observations within the site box (red line), the open ocean box (blue), or the sum of two boxes together (black).

While the data presented in Figures 9 and 10 are composites of many events, it is not hard to find individual events that embody the mean-pattern with thicker cloud over the Western Coast Range to the south, and less cloud to the north and east of Tasmania. Figure 11 shows an example of an open-cellular case for August 2008 and a closed cellular case from February of 2006. We note that in both examples, the low cloud mesoscale structure is similar over the site (northwestern tip of Tasmania) to the adjacent ocean. Over the course of the deployment, we expect to obtain measurements for similarly good cases that can be used for detailed LES modeling, and a significant number of events (days) with winds from west or southwest (6 to 12 each month) that can be used for statistical analysis.

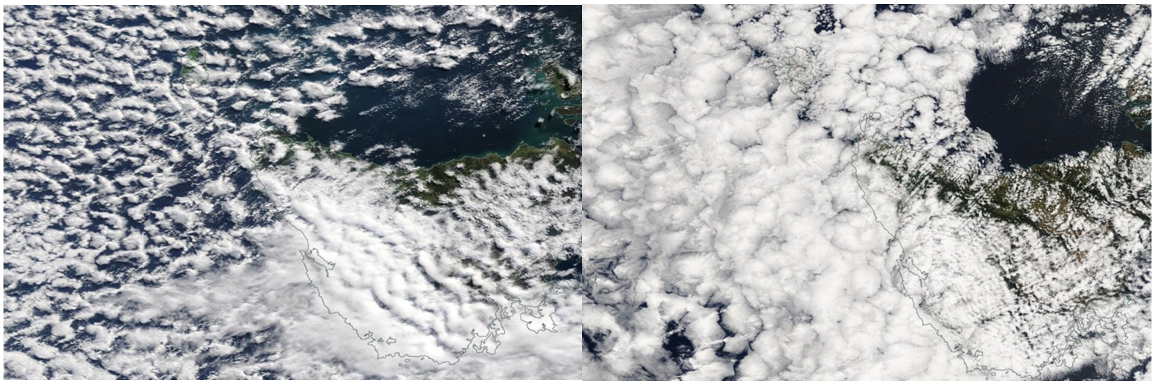

Figure 11. Cloud fields imaged by MODIS Terra on August 13, 2008 (left) and February 9, 2006 (right). Left panel shows open cellular structure typical of low clouds in the SH winter. Red depicts location of the site. Right panels show closed cellular mesoscale structure. In both examples, the low-cloud mesoscale structure is similar over the site (northwestern tip of Tasmania) to the adjacent ocean. The mesoscale structure is substantially disrupted by the higher coastal topography to the south and in the lee of the island, to the east.

Our overall conclusion is that there are relatively weak spatial gradients in cloud and precipitation occurrence at KCG, and to a much lesser degree in cloud-top temperature and cloud liquid water path at the site. However, differences between the site and the adjacent oceans are modest and small relative to the seasonal variations. This is particularly true for cloud effective radius and cloud droplet number concentration derived from MODIS data. We conclude that the CAPE-K deployment is likely to generate data that will be valuable in meeting the planned objectives.

Appendix B

KCG Logistics

KCG is located on the northwest tip of Tasmania 90 m above the sea surface. The station is bounded by the ocean to the SW and bordered by farmland (currently a dairy farm). The closest town is Smithton, where the BOM have an office. Access to the station is by road. The travel distance from Smithton is 50 km with approximately 40 km of the road being sealed. The final 10 km passes through the Woolnorth Dairy Farm and is unsealed road/track bounded by fenced fields. These tracks will have recently been traversed by heavy-lift cranes, so there should be no problem with trucks carrying a container.

- Security

The Kennaook/Cape Grim Baseline Air Pollution Station is surrounded by private rural land. Access is through a private farm, at the end of a rural road. This provides inherent security. Unwanted visitors are extremely rare. The building itself has monitored intrusion alarms.

- Freight

Several freight companies service Tasmania. Most equipment should be shipped to the Smithton BOM office. The freight address is 159 Nelson Street, Smithton, Tasmania 7330, Australia. The BOM Smithton office has a forklift for loading, and a van and small box trailer for transport.

Items requiring heavy transport or heavy lifting, such as containers, should be shipped directly to KCG. Each such item should be arranged in consultation with the Officer in Charge at KCG. Freight transport to Tasmania is typically best through the ports of Devonport or Burnie. The nearest aerodromes are on the north coast of Tasmania, in order of proximity Burnie/Wynyard (100 km), Devonport (170km), and Launceston (270km).

- Accommodation

Most visitors find accommodation at Smithton or the nearby seaside village of Stanley. There is a range of commercial accommodation available, noting busy summer seasons where forward bookings limiting short-notice availability. Both areas currently suffer a housing shortage, so bookings for long-term accommodation should be made well in advance.

- Electricity

The station is grid-connected with 3-phase 415 V (each phase 220-240 V) 50Hz power. There is a 100kVA generator onsite that automatically responds to outages with 9-second delay. Existing UPS circuits are fully utilized and not available.

- Personnel Support

Some simple first-in maintenance is possible by BOM technical staff, noting that existing staff are fully utilized with little spare capacity. Staff are typically present 10am to 4pm business days. Logistics advice and support will be offered. CSIRO may be able to help with personnel during IOPs and installation, etc.

- Communications

Mobile/cell communications is accessible on the Telstra network. Other networks have distant tower with sometimes-marginal connectivity. Land-line telephones are available at the station.

We are currently trialing Starlink services, which have proved to be functional and fast, and communications via this service may be available during the CAPE-K period.

Limited funding from ARM or Atmospheric System Research (ASR) will be requested for Co-PIs Mace and Marchand to provide scientific oversight, monitoring of the datastreams from CAPE-K, and participation in IOP activities. This would amount to a total ~$60K for travel and salary support during the deployment year. This aspect can be negotiated post-selection.

As part of this monitoring and to facilitate an initial publication for the purpose of community awareness, Mace and Marchand will compile routine statistics of the basic measurements and compare to similar statistics from other sites to ensure that the observations are physically reasonable. In addition, and as external funding allows, we will implement a few key retrieval algorithms that have already been developed using other ARM data sets, and which are not produced operationally by ARM. These algorithms will cover cloud and precipitation phase, cloud droplet number, etc. Monitoring such products, we will ensure consistency in the data sets. We also plan a BAMS-type publication to make the community aware of the CAPE-K data. Such a publication will require the basic statistics and initial algorithm results discussed in this paragraph. Funding for page charges of the BAMS article will be negotiated with ARM at an appropriate time if no other avenues exist for this purpose.

Appendix C

Routine Measurements at KCG

Property	Also known as	Instrument	Measurement frequency	Units
Particle number > 11 nm	CN, N11	TSI 3010 and TSI 3772	Minute, data reported as hourly	# cm^{-3}
Particle number > 2.5 nm (notionally)	UCN, N3	TSI 3756 (Installed on 29 November 2021)	Minute, data reported as hourly	# cm^{-3}
Particle number > 3 nm	UCN, N3	TSI 3776	Minute, data reported as hourly	# cm^{-3}
Aerosol size distribution	8.7-825 nm	MPSS	5 minute	dN/dlogDp # cm^{-3}
Cloud condensation nuclei > 750nm	CCN, 0.5% super saturation for hour 0-23, scanning SS for hour 24.	DMT CCN counter	Minute, data reported as hourly	# cm^{-3}
Cloud condensation nuclei > 750nm	CCN, 0.5% super saturation for hour 0-23, scanning SS for hour 24.	DMT CCN counter 2	Minute, data reported as hourly	# cm^{-3}
3 wavelength scattering coefficient (at 635, 525, 450nm)	σ_{sp}	Nephelometer	Minute, data reported as hourly	mM^{-1}
3 wavelength scattering coefficient (at 635, 525, 450nm); light scattering measurements from any angle between 10° and 90° up to 170°	σ_{sp}	Polar integrating nephelometer Aurora 4000	Minute, data reported as hourly	mM^{-1}
Light absorption at 1 wavelength (and black carbon)	σ_{ap} and BC	MAAP (Multi-angle aerosol absorption photometer)	Minute, data reported as hourly	µg m^{-3}
Light absorption at 3wavelengths (467, 528 and 652 nm)	σ_{ap} at three wavelengths	TAP (tricolor absorption photometer)	Minute, reported as hourly	mM^{-1}
light absorption at 7 wavelengths (370, 470, 520, 590, 660, 880, 950)	σ_{ap} at seven wavelengths	Aethalometer® Model AE33	Minute reported as hourly	mM^{-1}

Property	Also known as	Instrument	Measurement frequency	Units
PM10 mass and chemical composition	HVQuartz and HVEmfab	Ecotech 3000	Weekly, baseline	μg m^{-3}
PM2.5 mass and chemical composition	LVT	Partisol 2000	Weekly, baseline	μg m^{-3}
Continuous chemical composition (refractory species) particles less than 1 μm	ACSM	Tof-ACSM (time-of-flight Aerosol Chemical speciation monitor)		μg m^{-3}
Gaseous elemental mercury	Tekran	Tekran 2357 GEM Monitor	Minute	ng m^{-3}
Gaseous elemental mercury	Tekran	Tekran-2537 GEM Monitor B	Minute	ng m^{-3}
Gaseous elemental mercury	Tekran	Tekran-2537 GEM Monitor A		ng m^{-3}
Rainwater chemical composition		Eigenbot		

Appendix D

Measurements planned for the R/V *Investigator* May 2025 Voyage

Property	Instrument
Particle number >11 nm (N10)	TSI CPC 3772
Particle number > 7 nm (N7)	TSI CPC 3750
Particle number > 3 nm (N3)	TSI CPC 3776
Aerosol size distribution (<PM1)	TROPOS MPSS
Aerosol size distribution (<PM10)	TSI APS
Aerosol scattering	Ecotech Aurora 4000 nephelometer
Aerosol absorption	Magee aethelometer AE33
Black carbon concentrations	Thermo MAAP
Cloud condensation nuclei (CCN) number concentrations	DMT CCN-100
Aerosol chemical composition – real-time organic and inorganic species	Aerodyne ToF-ACSM
Aerosol chemical composition – integrated – mass, soluble ions, and elemental and organic carbon	Filter aerosol samplers (in triplicate, PM1 or PM2.5)
Aerosol optical depth	Microtops II sun photometer
Ice nuclei concentrations	IN filters
Standard meteorological parameters (e.g., wind speed, direction, temperature, humidity, etc.)	Meteorological packages (in duplicate, MNF)
Boundary-layer height	Mini-MPL
Sondes	3-5 times per day
W-Band radar reflectivity (zenith)	BASTA Doppler radar
W-Band Doppler velocity (zenith)	BASTA Doppler radar on stabilized platform
355 nm lidar attenuated backscatter	Raman lidar
23 and 31 GHz brightness temperatures	2-channel Radiometrics microwave radiometer
C-Band dual polarization radar volume scans	OceanPol radar
K-Band radar reflectivity	MRR2
Precipitation droplet size distribution	OceanRain disdrometer
Downwelling broadband solar and IR fluxes	Starboard and port pyranometers and pyrgeometers

www.arm.gov

U.S. DEPARTMENT OF ENERGY

Office of Science